### Universidad de Cuenca

Facultad de Ingeniería

Maestría en Hidrología mención en Ecohidrología

Hydrogeomorphology influence on pan-tropical transit times

Trabajo de titulación previo a la obtención del título de Magíster en Hidrología mención en Ecohidrología

#### Autor:

Fabián Leonardo Quichimbo Miguitama

#### **Director:**

Christian Birkel Dostal

ORCID: 00000-0002-6792-852X

Cuenca, Ecuador

2023-09-04



#### Resumen

Los trópicos son una de las regiones más diversas y dinámicas de la Tierra. A pesar de su importancia, nuestra comprensión de los procesos hidrológicos tropicales sigue siendo un desafío significativo, en su mayoría debido a la monitorización limitada. En este estudio, utilizamos conjuntos de datos isotópicos de alta resolución (diaria) de la entrada y salida de siete cuencas pan-tropicales en Australia, Costa Rica y Ecuador, para estimar y comparar tiempos de tránsito del aqua con variables hidrogeomorfológicas. Utilizando el método de la integral de convolución con una distribución gamma como función de transferencia, las cuencas pan-tropicales mostraron tiempos de tránsito entre 49 y 497 días, eficiencias de Kling Gupta alcanzadas de hasta 0.92. El parámetro alfa de la distribución gamma estuvo por debajo del patrón global previamente identificado de alrededor de 0.5 en 5 de las 7 cuencas. Un enfoque de ranking de bosque aleatorio (RF) identificó la capacidad de almacenamiento de agua y la cantidad anual de precipitación como los controles más importantes de los tiempos de tránsito. Además, la distribución de los tiempos de tránsito según lo indicado por el parámetro alfa se explicó mejor por la evapotranspiración anual, y la cobertura de suelo Andosol (%). Nuestros hallazgos identificaron los controles clave de los tiempos de tránsito y su distribución en cuencas tropicales de respuesta rápida en comparación con otras zonas geomorfológicas y climáticas, resaltando el valor de los tiempos de tránsito como un descriptor simple de la cuenca.

Palabras clave: trópicos, distribución de tiempos, isótopos estables, integral de convolución, distribución gamma





El contenido de esta obra corresponde al derecho de expresión de los autores y no compromete el pensamiento institucional de la Universidad de Cuenca ni desata su responsabilidad frente a terceros. Los autores asumen la responsabilidad por la propiedad intelectual y los derechos de autor.

Repositorio Institucional: https://dspace.ucuenca.edu.ec/



#### Abstract

The tropics are one of the most diverse and highly dynamic regions on Earth. Despite their importance, our understanding of tropical hydrological processes remains a significant challenge mostly due to limited monitoring. Here, we used high-resolution daily input-output isotope data sets from seven pan-tropical catchments ranging in size from 3 to 990 km<sup>2</sup>, located in Australia, Costa Rica, and Ecuador to estimate and compare streamflow transit times (TTs) with potential explanatory hydrogeomorphological variables. Pan-tropical catchments resulted in short TTs from 49 to 497 days using a simple lumped convolution integral model with a Gamma distribution as transfer function (best-fit Kling Gupta efficiencies up to 0.92). The gamma distribution alpha parameter was in 5 out of 7 catchments below the previously identified global pattern of around 0.5. A random forest (RF) ranking approach identified water storage capacity, the presence of sedimentary rocks (%), and the annual precipitation amount as the most important TT controls. In addition, the TT distribution as indicated by the alpha parameter was best explained by annual evapotranspiration, the soil texture, and the Andosol soil cover (%). Our findings identified the key TT and TT distribution controls in fast responding tropical catchments compared to other geomorphic and climate zones emphasizing the value of TT as a simple catchment descriptor.

Keywords: tropics, time distribution, stable isotopes, convolution integral, gamma distribution





The content of this work corresponds to the right of expression of the authors and does not compromise the institutional thinking of the University of Cuenca, nor does it release its responsibility before third parties. The authors assume responsibility for the intellectual property and copyrights.

Institutional Repository: https://dspace.ucuenca.edu.ec/



#### Índice de contenidos

R	esume	n		2
Α	bstrac	t		3
1.	Intro	duc	tion	7
2.	Data	١		9
	2.1.	Pan	-tropical study catchments	9
	2.2.	Hyd	rometeorological Data	9
	2.3.	Rair	nfall and streamflow isotope data	13
3.	Meth	ods		14
	3.1.	Cato	chment Characterization	14
	3.1.1	١.	Landscape variables	14
	3.1.2	2.	Geological variables	15
	3.1.3	3.	Hydrological variables	15
	3.2.	Trar	nsit Time estimations	16
	3.3.	Stat	istical analysis	18
4.	Resi	ults .		18
	4.1.	Hyd 18	rogeomorphology and isotope characteristics of the tropical study cate	chments
	4.2.	Trar	nsit time simulations and parameter uncertainty	23
	4.3.	Rela	ating transit times to pan-tropical catchment characteristics	26
5.	Disc	ussi	on	29
	5.1.	Pan	-tropical isotope characteristics and transit time estimates	29
	5.2.	Hyd	rogeomorphic drivers of pan-tropical transit times	30
6.	Con	clus	ions	31
R	eferen	ces .		33
Α	nnexes	S		44
	Annex	A.	Data source and descriptive statistics of isotopic signatures	44
	Annex	B.	Data records of all catchments	45
	Annex	C.	Exponential Model results	45
	Δηηρν	D	Correlation assumption	46



### Índice de figuras

<b>Figure 1</b> . Pan-tropical study catchments in Costa Rica; Ecuador and Australia using the pantropical band ±20° (Cai et al., 2019)
<b>Figure 2.</b> Precipitation and streamflow isotope variability (boxplots) and LMWLs of all pantropical catchments. Blue dots represent streamflow isotope signal. Blue lines represent the WL of streamflow. Orange dots are the precipitation isotope signal. Orange lines are the LMWL of precipitation samples. Gray line represents the Global Meteoric Water line (GMWL) $y = 8x+10$ as a reference.
<b>Figure 3.</b> Fitted deuterium signal simulations in streamflow using a convolution integral approach with a gamma model as transfer function: A-G: Deuterium signal simulations in streamflow. Measured streamflow isotope signal as blue points. 90% uncertainty bands in gray obtained from the retained parameter sets during calibration. H-N: Probability Density Functions (best-fit $\alpha$ and $\beta$ values) as gray line, and global PDF ( $\alpha$ = 0.5 and $\beta$ calibrated to the specific site) in red.
<b>Figure 4</b> . Spearman correlations. Alpha parameter ( $\alpha$ ) correlated with: A) percentage of Andosols, B) A group soil texture, C) altitude, D) mean annual evapotranspiration, E) percentage of months with zero precipitation, and F) coefficient of variation with monthly precipitation. MTT values correlated with: G) percentage of Andosols. H) percentage of igneous rock, I) percentage of sedimentary rock, J) mean annual precipitation, K) delta storage (term of the hydrological balance equation $\Delta$ sto = P-ET-Q), L) seasonality index, and M) percentage of days with zero precipitation. X-axis and y-axis errors are represented with horizontal and vertical lines respectively on each point of the scatter plots
<b>Figure 5.</b> Ranking important explanatory variables of MTT and alpha based on the %IncMSE for all predictors used in a Random Forest model



#### Índice de tablas

<b>Table 1.</b> Location, altitudinal range, area and sampling period of the study catchments together with climate (mean annual precipitation (P), mean annual streamflow (Q) and mear annual actual evapotranspiration (AET) and mean annual air temperature (T)), and geology (lithology, rock type and % cover)
Table 2. Catchment descriptors (hydrogeomorphology) used for correlation analysis with transit time estimations.         20
Table 3. The best-fit MTT estimations of all study catchments using two different models         Gamma (GM) and exponential model (EM) with the retained parameter range and median, as         well as the best fit MTT's, KGE efficiencies and references.
<b>Table 4</b> . Spearman correlation coefficients with significance values of alpha (α) and MT1 related to landscape, geology, and hydrologic variables



#### Hydrogeomorphology influence on pan-tropical transit times

#### 1. Introduction

The tropics play a crucial role in providing ecosystem services such as water production, carbon capture, and biodiversity (Barlow et al., 2018). However, the hydrological systems of the tropical region are highly dynamic, complex and challenging to understand and predict due to their heterogeneity. The high temporal and spatial rainfall variability, for example, results in extreme water and material fluxes (Macdonald et al., 2019; Wohl et al., 2012). Tropical systems have also co-developed under a diversity of geologic, climate, soil and biological conditions, contributing to highly variable characteristics. Additionally, population growth continuously changes the distribution of land cover and land use (Barlow et al., 2018; Bonell, 2005; Buytaert et al., 2002; Cai et al., 2019). The aforementioned factors and their complex interaction pose significant challenges to water management in the region (Blöschl et al., 2019). The challenges of water provisioning, hydrometeorological risk management, hydropower and aquatic ecological integrity are further exacerbated by a lack of understanding of the fundamental hydrological processes across the tropics (Wohl et al., 2012). Despite progress in certain countries, for example in terms of modelling (Arciniega-Esparza et al., 2023), a science and data-based water management is still hindered in many developing tropical countries due to the lack of crucial hydrometric data and monitoring.

Tracers emerged as an economic alternative and additional source of information to hydrometric data that can be particularly useful assessing the temporal response and transit times in tropical catchments (Birkel et al., 2016; Timbe et al., 2014). More generally, tracers provide insights into catchment transit times, stream water sources, flow pathways, and water storage (Knapp et al., 2019; McGuire & McDonnell, 2006; Stewart & McDonnell, 1991). Many studies focused on relating input-output tracer information with lumped convolution integral models (Maloszewski & Zubert, 1982) to estimate the mean transit time (MTT) as a catchment descriptor (see review by (McGuire & McDonnell, 2006)). The MTT showed to be strongly influenced by topography (McGuire et al., 2005), hydroclimate (Birkel et al., 2016), soil physical characteristics (Hrachowitz et al., 2009), urban impermeable surface area (Soulsby et al., 2014), and geologic controls (Cartwright et al., 2020), among other factors in different climatic and geomorphic settings.

Recognizing that transit times are non-stationary in nature (e.g., Klaus et al., 2015; Rinaldo et al., 2011 and a recent review by Benettin et al., 2022), new methods have emerged such as the Storage Age Selection (SAS) approach (Benettin et al., 2017) the young water fraction (Kirchner, 2016) or tracer-aided rainfall-runoff models that do not depend on an a priori TT distribution (see review by Birkel & Soulsby, 2015). However, the stationary lumped convolution integral models still find applications due to their simplicity and due to the almost universal gamma distribution (Godsey et al., 2009) converting the resulting catchment transit time distributions into useful descriptors, particularly for catchment comparative studies (Hrachowitz et al., 2010; Tetzlaff et al., 2009).

Although transit times have been estimated in tropical catchments, very few studies have reported potential relationships between catchments properties (i.e.: geology, hydrological variables, soil properties, etc.) and the TTD estimations. In humid tropical rainforests in Costa Rica, it was found that these systems are dominated by young waters with ages from hours to 3.3 years in drought situations, emphasizing the rapid rainfall-runoff and material transport dynamics (Birkel et al., 2016; Correa et al., 2020). In the cloud forest region of Mexico, MTTs of around 1.2 to 2.6 years were related to slope and permeability. The latter suggests that deep and long subsurface flow paths contribute to sustain base flow, particularly during dry periods (Muñoz-Villers et al., 2016). In Ecuador, the high regulation capacity and constant water supply of the paramo ecosystem depends on the catchment slope and the soil type, where shallow subsurface flow dominates resulting in short MTTs of less than 1 year (Larco et al., 2023; Mosquera et al., 2016). On the other hand, in a tropical montane catchment in eastern Kenya, a MTT of up to 4 years was estimated, mainly due to substantial groundwater contributions to streamflow throughout the year (Jacobs et al., 2018). However, a more systematic and comparative study on tropical transit times is still missing, but feasible with more higher resolution (daily) stable isotope time series made available.

Therefore, this study tested the gamma distribution as a lumped convolution integral model transfer function to examinate how its parameters vary in different catchments with variable landscape characteristics and climate conditions (Beven, 2010; McDonnell et al., 2010). We used data from tropical catchments in South America, Central America, and Australia to enhance our current knowledge of tropical hydrology, with the following specific objectives:

- i) estimate transit times and distributions of different pan-tropical catchments,
- ii) relate the TTDs to catchment characteristics in a catchment comparison exercise and,



iii) analyze the most important hydrogeomorphic drivers of transit times and their distributions.

#### 2. Data

#### 2.1. Pan-tropical study catchments

The pan-tropical region refers to the geographical area that extends approximately ±20 degrees northern and southern latitude from the equator and encompasses regions situated within the tropical belt of the Earth (Cai et al., 2019). In this region we analyzed hydrometric and isotopic data from seven catchments located in Australia (i.e., Howard and Atika), Costa Rica (i.e., Caño Seco, Quebrada Grande, Alberto Manuel Brenes-RBAMB and Tempisque) and Ecuador (i.e., Zhurucay) (Figure 1 and Table 1). The altitude range of all analyzed catchments was between 12 and 3788 m a.s.l., while their areas varied from 1.5 to 990 km².

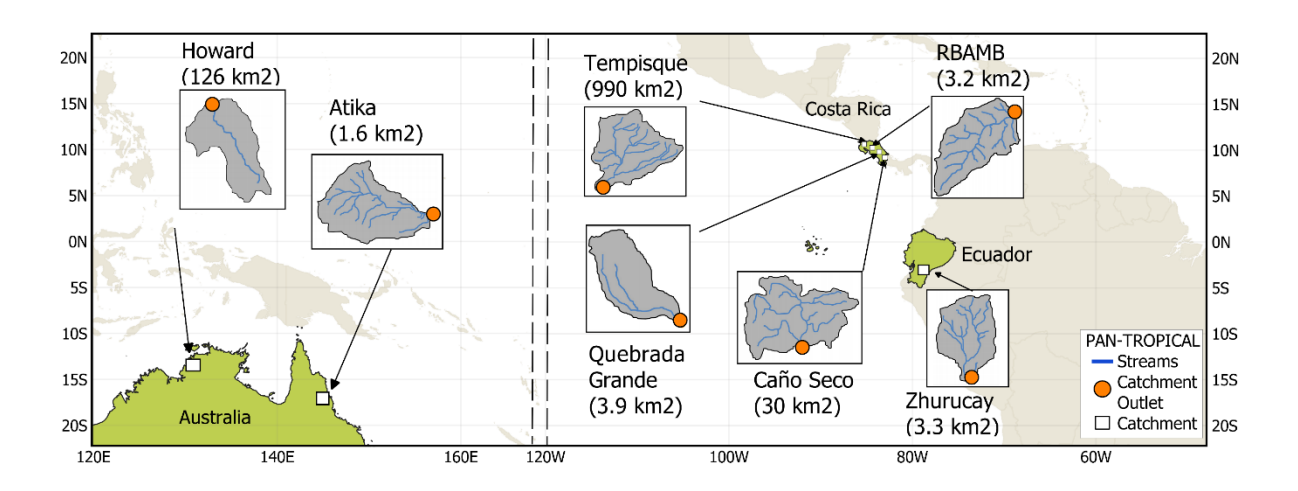


**Figure 1.** Pan-tropical study catchments in Costa Rica; Ecuador and Australia using the pantropical band ±20° (Cai et al., 2019).

#### 2.2. Hydrometeorological Data

Existing daily rainfall and discharge data, as well as temperature, relative humidity and evapotranspiration estimates were recompiled for the above presented pan-tropical catchments (footnotes of Table 1). The mean annual precipitation, streamflow, and actual evapotranspiration, exhibited ranges of 958 to 5116 mm year<sup>-1</sup>, 400 to 2100 mm year<sup>-1</sup> and 461 to 1338 mm year<sup>-1</sup>, respectively. Mean annual air temperature varies from 6 to 27 °C. The different tropical climates of our study catchments were identified using the updated Köppen-Geiger classification (Beck et al., 2018; Köppen, 1936; Peel et al., 2007) and include tropical savanna-Aw (i.e., Howard, Tempisque), tropical rainforest- Af (i.e., Atika, Caño Seco, Quebrada Grande, Alberto Manuel Brenes RBAMB), and tropical alpine biome without dry



season and cold summer-Cfc (i.e., Zhurucay). For more details on hydrometeorological characteristics of the study catchments see Table 1.

**Table 1.** Location, altitudinal range, area and sampling period of the study catchments, together with climate (mean annual precipitation (P), mean annual streamflow (Q) and mean annual actual evapotranspiration (AET) and mean annual air temperature (T)), and geology (lithology, rock type and % cover)

Catchment		Location	Altitude	Area	Sampling	*P	Q	**ET	т	***	Geolo	gy		
		(degrees)	(m a.s.l.)	(km²)	Sampling Period	(mm)	(mm)	(mm)	(°C)	Climate	FORMATION: Dominant Lithology	Class	Coverage (%)	
ralia	Howard	12°30'S 131°05'E	0-40	126	2015- 2018	1820 [1880]	758.5	1060 <sup>1</sup>	27	Aw <sup>8</sup>	DARWIN: Sandstone, Claystone <sup>15</sup>	Sedimentary	100	
Australia	Atika	16°49'S 145° 41'E	13-508	3.7	2019- 2021	2265 [1992]	618	1348 <sup>2</sup>	25	Af <sup>9</sup>	HODGKINSON: Mudstone, siltstone, conglomerates <sup>16</sup>	Metamorphic	100	
	Caño Seco	8°40'N	907-	30	2012-	2124	1325	799 <sup>3</sup>	20	Af <sup>10</sup>	TERRABAN: Lulitas, liltstones, pyrite sandstones, tuffaces, conglomerates, turbidities <sup>17</sup>	Sedimentary	58.9	
Costa Rica	Cano Seco	82°51'W	82°51'W 1475	82°51'W 1475 <sup>3</sup>	475	2014	[3052]	1323	199	20	Al	FILA DE CAL: Shallow limestone of reef platform <sup>18</sup>	Sedimentary	0.1
											AGUACATE: Andesite, basalts, gaps, tuffs <sup>19</sup>	Igneous	41	
Cost	Quebrada Grande	1°6'0''N 84°3'W	1765- 2350	3.9	2016- 2019	5117 [4000]	1596	612 <sup>4</sup>	27	Af <sup>11</sup>	QUEBRADA GRANDE: Basalts, Andesites <sup>20</sup>	Igneous	100	
	RBAMB	10°14′2″N 84°37′5″W	870- 1470	3.2	2013- 2017	2790 [2589]	2100	455 <sup>5</sup>	19	Af <sup>12</sup>	TERTIARY: Basalts, Andesites, pyroclastics flow <sup>21</sup>	Igneous	100	
	Tempisque	10.6°N 85.45°W	0-1900	990	2015- 2021	1800 [1920]	700	1100 <sup>6</sup>	27	Aw <sup>13</sup>	Volcanic rocks <sup>22</sup> Sediments <sup>23</sup>	Igneous Sedimentary	90 10	
Ecuador		3°04'S	2400			958.6					QUIMSACOCHA:Basaltic flows with plagioclases, feldespars <sup>24</sup>	Igneous	50	
	Zhurucay	79° 14'W	3400- 3900	3.3	2017- 2019	[1345]	433	461 <sup>7</sup>	7.6	Cfc <sup>14</sup>	TURI: Tuddaceous andesitic breccias, conglomerates, stratified sands <sup>25</sup>	Igneous	30	
											QUATERNARY:Sediments <sup>26</sup>	Sedimentary	20	



\*Mean Annual precipitation: long-term historic in brackets: [1989-2018] Australia, [> 5 years] Atika, [> 10 years] Caño seco, [1992-2003] Quebrada Grande River, [> 5 year] RBAMB, [1998-2020] Tempisque, [1964-2008] Zhurucay. \*\*Evapotranspiration method: 1 (AET) Eddy covariance flux tower, 2 (AET) (FAO-56), 3 (PET) (Hargreaves); 4 (AET) Penman-Monteith. 5 (PET) Penman-Monteith, 6 (AET) MODIS satellite, 7 (AET) Eddy covariance flux tower. \*\*\* Köppen-Geiger Clasification: 8 (Birkel et al., 2020), 9 (Duvert et al., 2022) 10 (Méndez & Molina Montero, 2016), 11 (Mayer-Anhalt et al., 2022), 12 (Martínez-Cuenca et al., 2020), 13 (Nauditt et al., 2022), 14 (Kannan et al., 2020). 15 (Cook et al., 1998; Doyle, 2001; Duvert et al., 2020); 16 (Bass et al., 2014; Blewett, 2012; Lim et al., 2022); 17,18,19 (Méndez & Molina Montero, 2016), 20 (Mayer-Anhalt et al., 2022; Sánchez-Murillo et al., 2019); 21 (Bergoeing, 2007; Correa et al., 2020; Dehaspe et al., 2018; Solano-Rivera et al., 2019); 22,23 (Erlich et al., 1996; Guzmán Arias & Calvo-Alvarado, 2012); 24,25,26 (Coltorti & Ollier, 2000; Longo & Baldock, 1982; Panagos et al., 2022; Pratt et al., 1997).

4



#### 5 2.3. Rainfall and streamflow isotope data

- 6 Streamflow samples in the Howard catchment were collected using 50 ml centrifuge tubes,
- 7 with a weekly frequency during wet seasons and monthly during dry seasons, as reported by
- 8 Birkel et al. (2020). Rainfall was collected daily using a dip-in rainfall sampler (RS-1C,
- 9 PALMEX, Zagreb-Croatia) designed to avoid evaporation (Gröning et al., 2012). All waters
- were filtered through 0.45 µm membrane on-site, then kept on ice and refrigerated upon arrival
- 11 to the laboratory. Stable isotope analysis was conducted using a Cavity Ring-Down
- 12 Spectroscopy (CRDSL Picarro L2130-i) with standard errors reported (±σ: ±0.5 ‰ for δ2H and
- 13  $\pm 0.1$  % for  $\delta 18O$ ).
- 14 In the Atika catchment (Lim et al., 2022), streamflow samples were collected using an
- 15 automatic water sampler (3700, Teledyne ISCO, Nebraska-USA) every week during non-
- events and every 2 hours during events. Rainfall samples were collected daily using a rainfall
- 17 sampler (RS-1C, PALMEX, Zagreb-Croatia). All water samples were stored in dark brown
- 18 glass bottles at room temperature in the laboratory prior to stable isotope analysis. Stable
- 19 isotope analysis was conducted using a Cavity Ring-Down Spectroscopy (CRDSL Picarro
- 20 L2130-i) with standard errors reported ( $\pm \sigma$ :  $\pm 0.5$  % for δ2H and  $\pm 0.1$  % for δ18O).
- 21 The Caño Seco (Birkel et al., 2016) streamflow samples were collected manually every two
- 22 days using a plastic funnel. Rainfall was collected daily using a passive sampler from a tipping
- 23 bucked rain gauge. In all water samples, a mineral oil was applied, and they were filled into
- 24 standard 3ml analytical vials and stored at 5°C. Stable isotope analysis was conducted using
- 25 a Liquid-Water Isotope Analyzer (DLT-100 Los Gatos) with standard errors reported (±σ: ±0.4
- 26 % for  $\delta$ 2H and  $\pm$ 0.1 % for  $\delta$ 18O).
- 27 The Quebrada Grande (Mayer- Anhalt et al., 2022), streamflow samples were automatically
- 28 collected daily using a Sigma 900 MAX (HACH, Iowa-USA) water sampler during 2016-2017,
- and manually with weekly frequency from 2017-2019. Rainfall was collected daily using an
- 30 on-site manual rainfall sampler (RS-1C, PALMEX, Zagreb-Croatia). All samples were stored
- 31 in 30 ml bottles at 5°C without headspace and were hermetically sealed to avoid exchange
- with atmospheric moisture. Prior to analysis, all samples were filtered using a 0.45 µm syringe
- 33 polytetrafluorethylene (PTFE) membrane. Stable isotope analysis was conducted using a
- 34 Cavity Ring-Down Spectroscopy (CRDSL Picarro L2120-i) with standard errors reported (±σ:
- 35  $\pm 0.5$  % for δ2H and  $\pm 0.1$  % for δ18O).
- 36 The RBAMB (Birkel et al., 2021) and Tempisque (unpublished) streamflow was sampled daily
- with an autosampler (3700, Teledyne ISCO, Nebraska-USA) and weekly, respectively, while

- 38 rainfall was collected daily at both sites using a rainfall sampler (RS-1C, PALMEX, Zagreb-
- 39 Croatia). All water samples were stored using 3-I plastic bottles using a funnel and inlet tube.
- Water samples were stored in 50-ml polypropylene, sealed with screw caps and later stored
- 41 in a fridge at 5°C, then filtered through 0.45 µm syringe polytetrafluorethylene (PTFE)
- 42 membrane. Stable isotope analysis was conducted using a Cavity Ring-Down Spectroscopy
- 43 (CRDSL Picarro L2120-i) with standard errors reported ( $\pm \sigma$ :  $\pm 0.5$  % for  $\delta 2H$  and  $\pm 0.1$  % for
- 44 δ18Ο).
- 45 In Zhurucay (Pesántez et al., 2023), streamflow was sampled every 4 hours using an
- autosampler (PVS4100D, Campbell, Utah-USA). Rainfall was collected for every 2.08 mm of
- 47 rain. The collected water was stored un 2mL amber glass bottles, covered with parafilm, and
- 48 kept away from the sunlight. Stable isotope analysis was conducted using a Cavity Ring-Down
- 49 Spectroscopy (CRDSL Picarro L2130-i) with standard errors reported (±σ: ±0.5 ‰ for δ2H and
- $\pm 0.1$  % for δ18O).
- We report all the isotope analysis equipment and its standard errors in Annex A. All rainfall
- 52 samples were collected daily with some sub-daily event sampling at RBAMB and Zhurucay.
- 53 The sub-daily samples were aggregated to a representative daily sample and standard model
- application across the tropical study catchments.

#### 55 3. Methods

56

57

58 59

60

61

62

63 64

65

66

67

68

69 70

#### 3.1. Catchment Characterization

#### 3.1.1. Landscape variables

The landscape characteristics such as the soil types and their relative percentage cover in each catchment were determined from the literature. Soils described in another soil classification system (e.g., Australian soil classification) were reclassified according to Krasilnikov et al. (2009) for a standard comparison with the Food and Agriculture Organization of the United Nations guides (FAO) (Driessen, 2001). The Howard catchment exhibits dominant Dermosols, Cambisols 73% and Fluviosols 27% (Brocklehurst, 2012). The Atika presents brown and red Dermosols as dominant soil types (Cambisols) (Murtha, 1986). Caño Seco's dominant soils are Andosols 66% and Alisols 34% (Méndez & Molina Montero, 2016). In Quebrada Grande, Andosols are the principal soil type with 100% cover (Mayer-Anhalt et al., 2022). RBAMB presents Andosols 80% and Cambisol 20% (Correa et al., 2020; Dehaspe et al., 2018). In Tempisque, Entisols (Regosols) 56% and Inceptisols (Cambisol) 34% predominate (Guzman & Calvo, 2013), and Zhurucay presents Andosols 74%, Histosols 22% and Leptosols 4% (Quichimbo et al., 2012).

The soil texture class was determined based on previous results from on-site soil profile descriptions. Furthermore, we compared the local measurements with the approach by Ross et al. (2018), who performed a global classification of soils using a 250 m grid size, with an emphasis on hydrologic and texture characteristics (FAO, 2006). Topographic variables such as average slope in percent, area in square kilometers and mean altitude in meters were estimated based on digital elevation models (DEMs) from Atika (Lim et al., 2022), Howard (Birkel et al., 2020; Duvert et al., 2020), Caño Seco (Birkel et al., 2016; Méndez & Molina Montero, 2016), Quebrada Grande (Mayer- Anhalt et al., 2022), RBAMB (Birkel et al., 2021), Tempisque (Venegas-Cordero et al., 2021) and Zhurucay (Mosquera et al., 2016) (Table 3).

#### 3.1.2. Geological variables

The geology of Howard catchment constitutes of the Darwin formation with Quaternary-Claystone and a sedimentary lithology (Cook et al., 1998; Doyle, 2001; Duvert et al., 2020). Atika belongs to the Devonian-Hodkinson formation conformed of primarily metamorphic rocks (Blewett, 2012; Lim et al., 2022). The Caño Seco belongs to three formations, the Terraba-Miocene (Denyer & Kussmaul, 2000), Fila de Cal-Eocene (Moya Arguedas, 1990) and Aguacate-Pliocene (Moya Arguedas, 1990) with dominant sedimentary and igneous lithology respectively. Quebrada Grande belongs to the Cenozoic-Miocene with dominant igneous lithology (Sánchez-Murillo et al., 2019). The RBAMB belongs to Tertiary formations with dominating igneous rocks (Bergoeing, 2007). The Tempisque exhibits Cenozoic- quaternary geology with igneous and sedimentary rocks (Erlich et al., 1996). The Zhurucay catchment belongs to the Quimsacocha-Miocene and Turi-Miocene formations, quaternary deposits with igneous and sedimentary rocks (Coltorti & Ollier, 2000; Longo & Baldock, 1982; Pratt et al., 1997). More details on the dominant lithology are presented in Table 1.

#### 3.1.3. Hydrological variables

Hydrometeorological variables such as the runoff coefficient, annual precipitation, annual actual evapotranspiration, and annual streamflow were obtained from the daily hydrometeorological data sets. Delta storage was estimated from the annual water balance as the difference between the input (precipitation) and outputs (evapotranspiration, streamflow), in percentage. We further used the seasonality index (SI) (Eq-1):

100 
$$SI[-] = \frac{1}{R_i} \sum_{j=1}^{12} \left| M_{ij} - \frac{R_i}{12} \right|$$
 Eq-1

where,  $R_i$  is the annual rainfall for the year i,  $M_{ij}$  is the monthly rainfall for month j. SI ranges from 0 (Non seasonal, all months with equal rainfall) to 1 (Extremely seasonal, all annual



rainfall occurs in one month) (Walsh & Lawler, 1981). The replicability index (RI) to assess variability of rainfall regimens (Eq-2):

$$RI [-] = \frac{SI_a}{SI_{mean}}$$
 Eq-2

where,  $SI_a$  is the seasonality Index at year a,  $SI_{mean}$  is the mean seasonality index of the whole period. High values for wet and dry months frequently occur at the same period every year. Small values indicate highly variable timing of wet and dry seasons (Walsh & Lawler, 1981). Percentage of days with zero precipitation (Eq-3):

110 
$$Day0 [\%] = \frac{\# Days_{p=0}}{\# Total \ days}$$
 Eq-3

- 111  $\# Days_{p=0}$  it the numbers of days of the whole monitored period with zero precipitation.
- # Total days is the total number of days over the monitored period. Precipitation not registered
- by the rain gauge with respect to the total number of days over the monitored period.
- 114 Coefficient of variation in daily precipitation PVAR (Eq-4):

115 
$$PVAR [mm/mm] = \frac{\sigma_P}{P_{mean}}$$
 Eq-4

- where  $\sigma_P$  is the standard deviation of daily precipitation,  $P_{mean}$  is the average of the daily
- 117 precipitation. Standard deviation of daily precipitation over the mean daily precipitation.
- 118 Months with zero precipitation (Eq-5) relative to the entire analysis period:

119 
$$Month0 [\%] = \frac{\# Months_{P=0}}{\# Total Months}$$
 Eq-5

- where, # months P=0 is the number of months with zero precipitation. # Total Months is the
- 121 number of total months of the whole period available. Monthly precipitation not registered by
- the rain gauge with respect to the total number of months over the monitored period.
- 123 Coefficient of variation in daily precipitation (Eq-6):

124 
$$PMVAR [-] = \frac{\sigma_{MP}}{P_{Mmean}}$$
 Eq-6

- where,  $\sigma_{MP}$  is the standard deviation of the monthly precipitation.  $P_{Mmean}$  is the average
- 126 monthly precipitation. [-] dimensionless. Standard deviation of monthly precipitation over the
- mean monthly precipitation.
- 128 3.2. Transit Time estimations
- We used the lumped convolution approach to estimate TTs in pan-tropical catchments. The
- 130 simple convolution integral transit time model (Eq-7) estimates stream isotopes ratios with

131

132

133134

135136

137

corresponding transit time, using a transfer function  $g(\tau)$  (Amin & Campana, 1996; Maloszewski & Zuber, 1982). This model converts the input of daily isotopic composition of precipitation into an approximation of the stream isotope ratios  $\delta_{out}(t)$ . The daily evapotranspiration was subtracted from the daily precipitation amount for the input function  $\delta_{in}(t-\tau)$ , assuming no fractionation of surface waters. This assumption is supported by the stream water isotope samples plotting consistently close to the calculated Local Meteoric Water Lines (LMWL) (See Figure 3).

Two transfer functions were applied here. 1) The gamma distribution model (GM) Eq-8 which is more flexible and a general version of the exponential model. The product of the two parameters ( $\alpha$ (-) is the shape parameter and  $\beta$ (days) the scale parameter) gives the MTT  $\tau$  (days) of the system (Hrachowitz et al., 2009). The Gamma model GM equation is:

$$GM = \frac{\tau^{\alpha-1}}{\beta^{\alpha}\Gamma(\alpha)} \exp\left(-\frac{\tau}{\beta}\right)$$
 Eq-7

- where the parameters  $\alpha$  and  $\beta$  ranged from 0.01 to 4 (-) and from 0 to 1825 (days) respectively.
- Due to the limitations of stable water isotopes to detect transit times exceeding 5 years
- 145 (Stewart et al., 2010), the scale parameter was limited to 1825 days (5 years).
- 146 2) The exponential model (EM) Eq-8 as a special case of the Gamma model represents a
- 147 well-mixed system and assumes contributions from all flow paths. This model uses one
- 148 parameter  $\tau$  and is described in Eq-8:

$$EM = \frac{1}{\tau} * \exp\left(-\frac{t}{\tau}\right)$$
 Eq-8

- 150 where  $\tau$  ranged from 0 to 1825 days.
- 151 For all catchments, we used a warm-up period prior to calibration that consisted in 5 times the
- measurement record resulting in a standardized calibration approach (Hrachowitz et al.,
- 153 2013). The gamma model and exponential model were calibrated for the periods shown in
- 154 Annex B. A qualitative validation compared our TT results to TTs reported for the same
- 155 catchments.
- 156 The calibration and evaluation of the TTD models was performed using the Differential
- 157 Evolution algorithm (DEoptim R package) developed by Ardia et al. (2011). The algorithm was
- implemented in R (R Core Team, 2021) and the performance of the gamma and exponential
- model was evaluated using the Kling-Gupta Efficiency criterion (KGE) (Gupta et al., 2009).
- 160 The KGE ranges from -∞ to 1, where unity indicates an ideal optimization. The calibration

procedure used a maximum of 10 000 iterations with a stop criterion for KGE of 0.01, and the simulations were presented with 90% percentiles uncertainty bands for the best performing 100 parameters sets. Efficiency values greater than 0.3 were considered acceptable (Knoben et al., 2019).

#### 3.3. Statistical analysis

We initially conducted a correlation analysis relating the estimated MTTs and TTD characteristics with hydroclimatic and landscape parameters using the non-parametric Spearman's rank correlation analysis (Wissler, 1905): 1) Landscape (soil type, soil texture and topographic features), 2) geological (rock type), and 3) hydrological (meteorological indices) parameters. The robustness of correlations was checked following these assumptions (Osborne & Waters, 2002; Williams et al., 2013): linearity, assessed by examining whether the mean of the residuals of each correlation is equal to or approximately zero (Pedhazur, 1997); normality, assessed using the Shapiro test to determine the normal distribution of the residuals (King & Eckersley, 2019); homoscedasticity, checked using the Score Test for Non-Constant Error Variance (ncv) (Cook & Weisberg, 1983); and the independence of the variables with the Durbin Watson test (Savin & White, 1977). All correlations and the hypotheses test were conducted using *lawstat* (Gastwirth et al., 2023) and *gvlma* (Peña & Slate, 2006) libraries using the R statistical programming language (R Core Team, 2021).

Furthermore, the identified drivers associated to MTTs and the TTD alpha parameter by correlation (p-value < 0.1), were ranked according to the relative importance using a random forest (RF) analysis (Liaw & Wiener, 2001). For the RF we used the increased mean square error (IncMSE) as a measure explaining the effect of an explanatory variable on the predicted result. Therefore, higher IncMSE values more positively impact on the target variables (MTTs and alpha values) (Breiman, 2001). The analysis was performed using the *randomForest* library implemented in R (Liaw & Wiener, 2001).

#### 4. Results

4.1. Hydrogeomorphology and isotope characteristics of the tropical study catchments

The pan-tropical catchment characterization is based on the landscape and hydrometeorological variables presented in Table 2. Here, we give a brief summary of the main characteristics. Four of seven catchments presented Andosol (Caño Seco, Quebrada Grande, RBAMB, Zhurucay) and Cambisol (Howard, Atika, RBAMB, Tempisque) soil types with more than 66% and 20% of the catchment area, respectively. Soil types such as Alisols

34% (Caño Seco), Histosols 22% (Zhurucay), Regosols 56% (Tempisque), and Fluviosols 27% (Howard) were the least abundant. The predominant soil texture groups are A (Sand) and B (Sandy Loams, Loamy Sands) in most of the catchments. According to the catchment size classification by Singh (1991), our catchments range from micro-catchments < 10 km² (Atika, Quebrada Grande, RBAMB, Zhurucay), small catchments < 100 km² (Caño Seco) to medium catchment size <1000 km² (Howard, Tempisque). The largest catchments (Howard and Tempisque) exhibited on average "sloping land" (10% - 15%), while the smaller catchments (Atika, Caño Seco, Quebrada Grande, RBAMB, and Zhurucay) are also the more mountainous and "moderately steep" (15% - 30%). The mean altitude covered a range from 12 to 3,788 m a.s.l. (Table 2). The geology of most of the catchments is dominated by ingenious rocks, with sedimentary rocks present to a lesser extent. The Atika is the only catchment with predominant metamorphic rocks (Table 2).

The mean annual precipitation, streamflow, and actual evapotranspiration in the catchments ranged from 959 to 5116, 433 to 2100 and 461 to 1060 mm year<sup>-1</sup>, respectively. Such a wide range shows the high hydrometeorological variability that characterizes the tropics (Cai et al., 2019). The wettest catchment Quebrada Grande, in Costa Rica, received the largest amount of precipitation (5116 mm year<sup>-1</sup>) and the RBAMB the highest streamflow (2100 mm year<sup>-1</sup>). The Australian Atika catchment registered the highest actual evapotranspiration (1348 mm year<sup>-1</sup>). The Zhurucay exhibited the lowest precipitation and streamflow (959 and 433 mm respectively) among all catchments. Most catchments are relatively humid (RH > 90%), except for the seasonally-dry Howard (RH ~ 65%). The mean annual temperature of all catchments is around 19.7 °C, except for the high-elevation Zhurucay (7.6°C). The runoff coefficients (RC) ranged from 0.27 to 0.75 with prominent overland and shallow subsurface flow. The water storage capacity in the catchments is relatively small (less than 10%) apart of the Quebrada Grande with a significant water storage capacity of 56% (Table 2).

The seasonality index reflected different tropical precipitation regimes from non-seasonal (Quebrada Grande, 0.2-0.39, Day0 < 30%) to more seasonal precipitation with a short dry season (SI: 0.4-0.59, Day0 < 60%) as in Caño Seco, RBAMB and Zhurucay. The Tempisque, Howard and Atika show a predominantly seasonal precipitation regime (SI: 0.6-0.79, Day0 < 30%, SI: 0.8-0.99, Day0 < 30%) with a long dry season of a minimum of four months. The replicability index shows high values when wet and dry months frequently occur at the same period every year (e.g., Howard). Conversely, small RI values suggest high variability in timing of the wet and dry season (e.g., Quebrada Grande). The percentage of months with zero precipitation (Month0) is less than 30% in all the catchments, and the coefficient of variation (PMVAR) is less than 1.27. The variability of daily precipitation (PVAR) is low in Tempisque

231

232

229 and Zhurucay, where PVAR < =0.6, but high in Howard and Caño Seco, where PVAR > 2 230 (Table 2).

**Table 2.** Catchment descriptors (hydrogeomorphology) used for correlation analysis with transit time estimations.

	Parameter	Howar d	Atika	Caño Seco	Quebra da Grande	RBAM B	Tempisqu e	Zhuruca y
	Andosol (%)	0	0	66	100	80	0	74
S	Cambisol (%)	73	100	0	0	20	34	0
Soil types	Alisoles (%)	0	0	34	0	0	0	0
	Histosol (%)	0	0	0	0	0	0	22
Ň	Regosol (%) Fluviosol	0	0	0	0	0	56	0
	(%)	27	0	0	0	0	0	0
<b>=</b> 3	A (%)	27	0	66	100	80	0	74
*Soil Textu	B (%)	73	100	0	0	20	34	4
* <b>⊢</b>	C (%)	0	0	34	0	0	56	22
iphi Ies	slope (%)	10.00	27.00	20.79	16.90	22.30	10.50	18.00
Topographi c variables	Area (km²)	126.00	1.57	31.21	3.90	3.20	990.00	3.28
Topographi c variables	Altitude (m a.s.l)	12	20	1037	2222	1133.5 0	260	3788
>	Igneous (%)	0	0	41	100	100	90	80
**Geology	Metamorphi c (%)	0	100	0	0	0	0	0
*	Sedimentary (%)	100	0	59	0	0	10	20
	P (mm year <sup>-1</sup> )	1819.1 0	2265.0	2123.8 7	5116.9 0	2790.0 0	1880.00	958.60
gical	AET (mm year <sup>-1</sup> )	1060	1348	799	612	455	1100	461
***Hydrometeorological variables	Q (mm year <sup>-1</sup> )	759	618	1325	1596	2100	700	433
ometeorc variables	RH (%)	65.70	82.00	95.30	95.00	96.30	95.00	92.00
'dro ∞	T (°C)	26.70	25.00	19.90	27.00	19.70	27.00	7.60
<b>H</b> ***	Delta Storage (%)	0.00	13.20	0.01	56.85	8.42	4.26	6.74
	RC (-)	0.42	0.27	0.62	0.31	0.75	0.37	0.45
			0.04	0.58	0.24	0.46	0.78	0.45
u	SI (-)	0.93	0.84	0.50	0.2 .		01.0	0.10
ason	SI (-) RI (-)	0.93 1.01	0.84	0.90	0.58	0.79	0.93	1.09
****Season al and								



Month0 (%)	27	6	3	0	1	29	0
PMVAR	1.19	1.27	0.80	0.50	0.69	1.11	0.55

<sup>\*</sup>A (Sa) sand; B (SaLo) Sandy Loam, (LoSa) Loamy Sand; C (CILo) Clay loam, (SiCILo) Silty clay loam, (SaCILo) Sandy clay loam, (Lo) Loam, (SiLo) Silty Loam, (Si) Silty. Classification done according to (Ross et al., 2018). (-) Dimensionless.

Figure 2 shows the Local Meteoric Water Lines (LMWL) for each site. The slope of the precipitation isotopic signal ranged from 7.7 to 8.3, with an average of 7.91±0.27, similar to the Global MWL. The intercept ranged from 6.5 to 16, with an average of 12.6±3.6 ‰. The slope of the regression equations for the streamflow signal reflected the internal processes of each catchment, with values ranging from 5.1 to 8.3, and an average of 6.6±1.34, while the intercept range was between -7.3 to 16, with an average of 4±8.84 ‰. The deuterium-excess parameter defined as d =  $\delta^2$ H -  $8^*\delta^{18}$ O varied between 8.79 and 14.6 for precipitation and between 9.9 and 16 for streamflow. Generally, the LMWLs show limited evaporation processes or mixing with other water sources. The boxplots in Figure 2 show the isotopic variability in precipitation and streamflow for oxygen-18 ( $\delta^{18}$ O) and deuterium ( $\delta^2$ H). The direct comparison of precipitation with streamflow variability is indicative of the degree of catchment filtering where a similar variability reflects little to no mixing and filtering. The Atika and Quebrada Grande show the highest input to output ratio.

<sup>\*\*</sup>Igneous (basaltics flows with plagioclases, feldspars, andesitic pyroclastics); Metamorphic (Mudstone, siltstone, conglomerates); Sedimentary (Shallow limestone of reef platform, lulitas, siltstones, sandstones, turbidities, pyrite).

\*\*\*Runoff coefficient (RC); precipitation (p); evapotranspiration (et); streamflow(q); relative humidity (RH); temperature (T); percentage of storage water (Δ storage)

<sup>\*\*\*\*</sup>Seasonality Index (SI); Replicability Index (RI); Percentage of days with zero precipitation (Day0), Coefficient of variation with daily precipitation (PVAR), Percentage of month with zero precipitation (Month0), coefficient of variation with monthly precipitation.



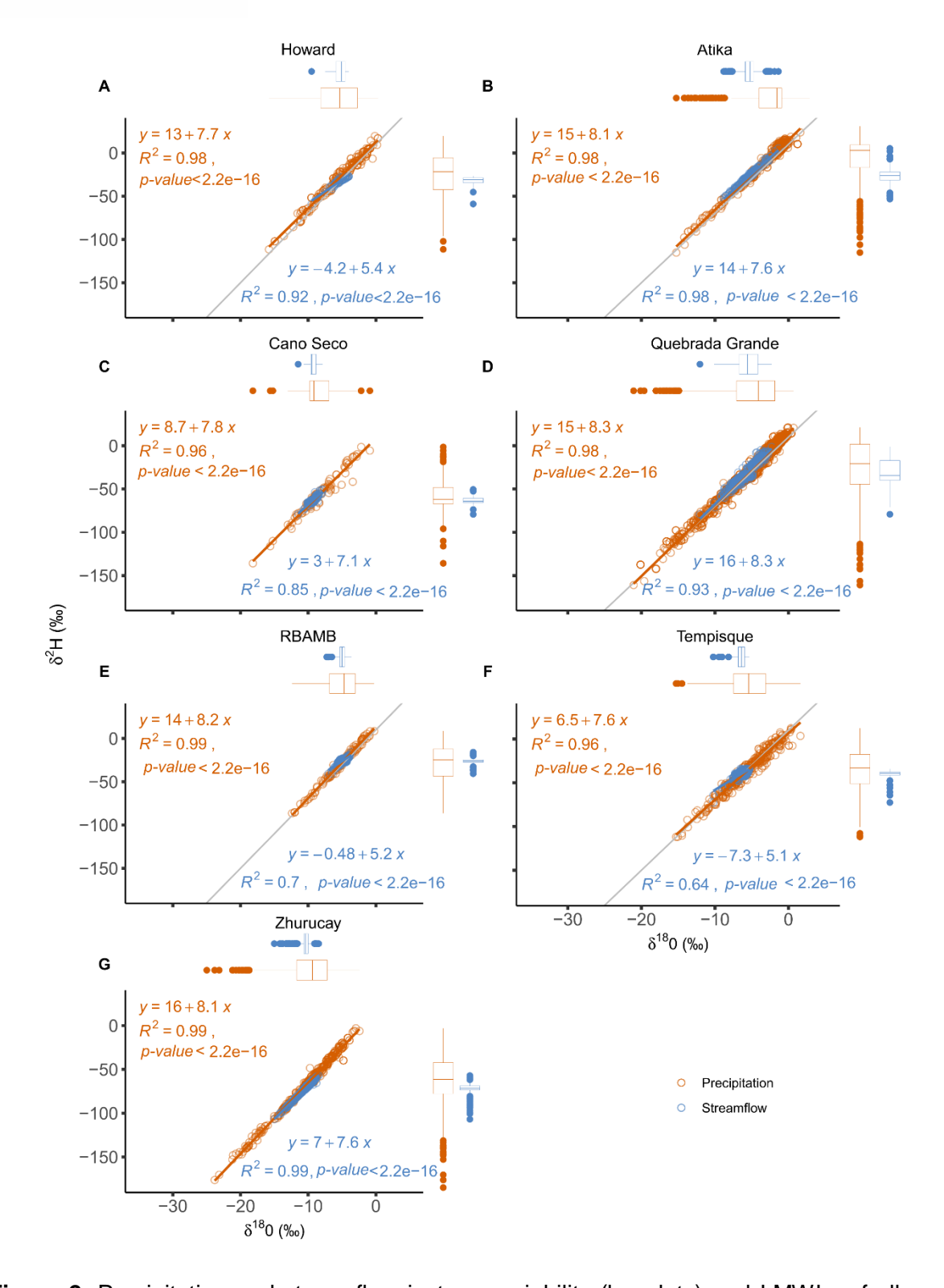


**Figure 2.** Precipitation and streamflow isotope variability (boxplots) and LMWLs of all pantropical catchments. Blue dots represent streamflow isotope signal. Blue lines represent the WL of streamflow. Orange dots are the precipitation isotope signal. Orange lines are the LMWL of precipitation samples. Gray line represents the Global Meteoric Water line (GMWL) y = 8x+10 as a reference.



#### 4.2. Transit time simulations and parameter uncertainty

The Howard, Caño Seco, and Tempisque catchments exhibited the longest MTTs (307 < MTTs < 495 days) compared to Atika, Quebrada Grande, RBAMB and Zhurucay (82 < MTTs < 252 days). When using the gamma model, the reported MTTs < 1.4 years were modelled with KGEs efficiencies ranging from 0.32 to 0.92 (Table 3). In comparison, the calibrated exponential model resulted in shorter MTTs < 0.4 years with lower KGEs efficiencies from 0.16 to 0.88. Table 3 summarizes the gamma and exponential model parameters, as well as the best-fit MTT's and KGE's.

**Table 3.** The best-fit MTT estimations of all study catchments using two different models. Gamma (GM) and exponential model (EM) with the retained parameter range and median, as well as the best fit MTT's, KGE efficiencies and references.

		GM			EM			
Catchme nt	Alpha (Range) calibrat ed	Beta (Range) calibrate d	MTT (Simulate d) Best fit	KG E	MTT (Simulate d) Best fit	KG E	M.	RENCES TT/TT days)
Howard- AUS	(0.2-0.3) 0.27	(944- 1825) 1825	(283-497) 494.83	0.6 1	(113-124) 123.46	0.1 8	~511	(Birkel et al., 2020)
Atika- AUS	(0.12- 0.18) 0.18	(1034- 1318) 1115.02	(49 -228) 197.00	0.8 4	(28-113) 53.37	0.6 7		
Caño Seco- CRI	(0.16- 0.22) 0.19	(1213- 1552) 1535	(274-340) 336.70	0.6 3	(109-113) 104.2	0.3 8	~213	(Mendez et al., 2016)
Quebrad a Grande- CRI	(0.22- 0.44) 0.42	(179- 389) 195.70	(80-151) 81.74	0.9 2	(69-113) 72.52	0.8 8	~87	(Mayer- Anhalt et al., 2022)
RBAMB- CRI	(0.52- 0.65) 0.64	(248- 323) 259.57	(130-438) 165.69	0.3 9	(113-157) 156.20	0.3 7	~162	(Correa et al., 2020)
Tempisqu e-CRI	(0.16- 0.22) 0.18	(1730- 1825) 1825	(289-438) 322.19	0.3 2	(82-113) 85.53	0.1 6		
Zhurucay -ECU	(0.6- 0.66) 0.63	(382- 412) 400	(229-264) 252.02	0.7 6	(113-230) 163.12	0.5 7	~188	(Mosque ra et al., 2016)

264 -- No previous reported values.

The gamma model reliably represented the extremes of the isotopic signals (Figure 3: Panels A-G KGE<sub>gamma</sub> > 0.32) and resulted in better fits compared to the exponential model (Annex C: Panels A-G, KGE<sub>exponential</sub> > 0.16). Therefore, we used the GM MTT results in further

statistical analysis. The Probability Density Functions (PDFs) in Figure 3, panels H-N, were
plotted with the best-fit GM parameters ( $\alpha$ and $\beta$ ), and a normalized scale [0,1]. The latter
resulted relatively similar to the global PDF ( $\alpha=0.5$ and $\beta=$ beta calibrated to the specific
site).

272

268269270271

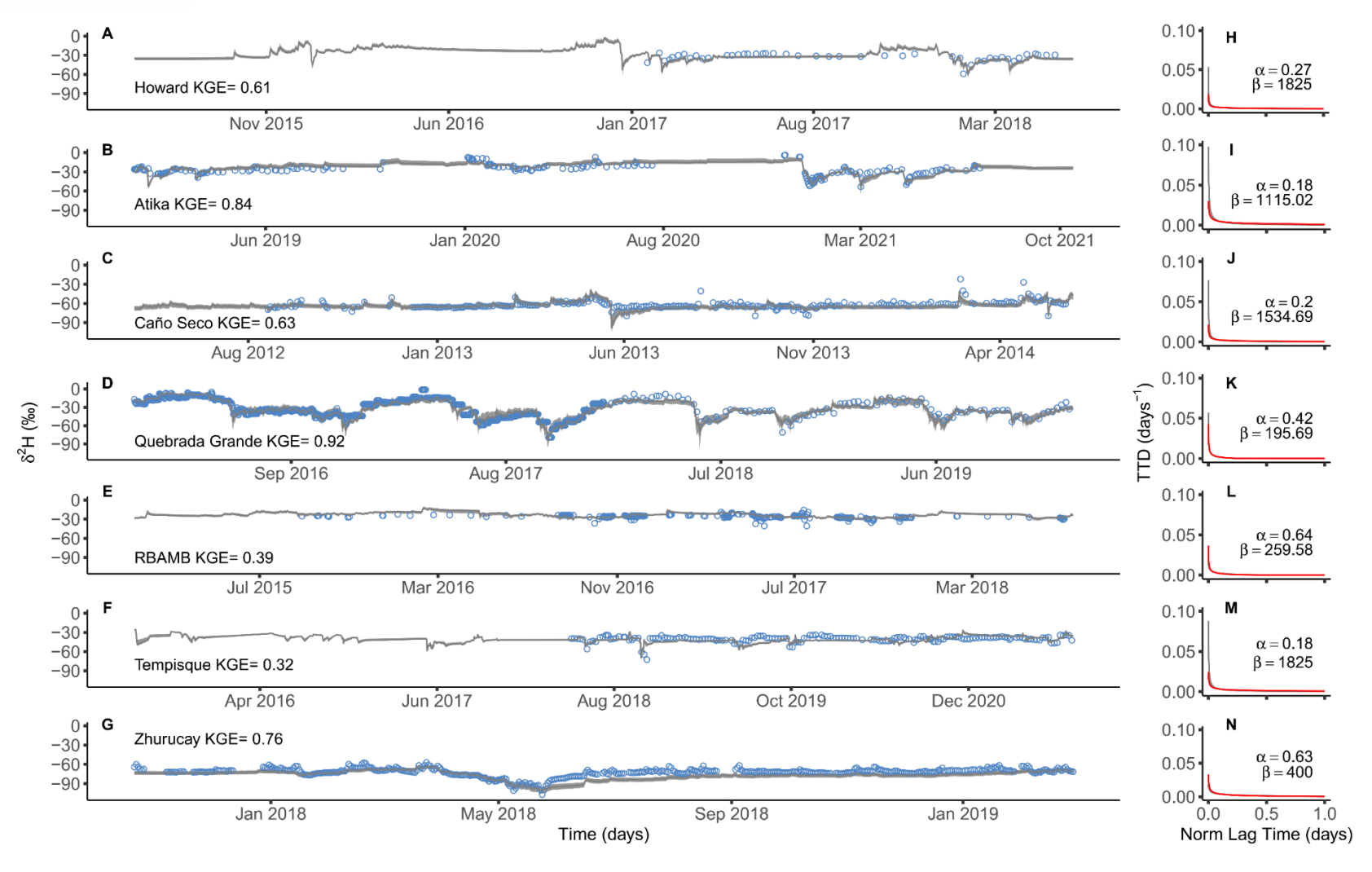


**Figure 3.** Fitted deuterium signal simulations in streamflow using a convolution integral approach with a gamma model as transfer function: A-G: Deuterium signal simulations in streamflow. Measured streamflow isotope signal as blue points. 90% uncertainty bands in gray obtained from the retained parameter sets during calibration. H-N: Probability Density Functions (best-fit α and β values) as gray line, and global PDF ( $\alpha = 0.5$  and β calibrated to the specific site) in red.

Fabián Leonardo Quichimbo Miguitama

#### 4.3. Relating transit times to pan-tropical catchment characteristics

The nonparametric Spearman rank correlation was used to relate the calibrated alpha parameters and the resulting MTTs (Table 3) from the GM of all catchments to the hydrogeomorphological catchment characteristics from Table 2. Such correlations revealed which variables were influencing water age and allowed inference on how (Table 4). The statistically robust and significant correlations (p-value < 0.1) are presented in Table 4 and Annex D. Figure 4 shows the positive correlations of the alpha parameter with Andosol soils (Figure 4-A, r = 0.79), soils texture (Figure 4-B, r = 0.85) and mean altitude (Figure 4-C, r = 0.67). Negative correlations resulted with the actual evapotranspiration (Figure 4-D, r = -0.96). percentage of months with zero precipitation (Figure 4-E, r = -0.75), and the coefficient of variation with monthly precipitation index (Figure 4-F, r = -0.72). The MTTs correlated with the percentage of sedimentary rocks coverage (Figure 4-I), seasonality index (Figure 4-L), and percentage of days with zero precipitation (Figure 4-M). Conversely, variables as the percentage of Andosols coverage (Figure 4-G), percentage of igneous rocks coverage (Figure 4-H), mean annual precipitation (Figure 4-J), and water storage catchment capacity (Figure 4-K) negatively correlated with MTTs (p-value < 0.098). The other variables only exhibited weak correlations with MTTs and the alpha parameter (Table 4).

**Table 4.** Spearman correlation coefficients with significance values of alpha (α) and MTT related to landscape, geology, and hydrologic variables.

	Soil Type	Alpha	MTT	
	Andosol	0.79(0.036)	-0.7(0.077)	
	Cambisol	-0.6(0.154)	0.34(0.452)	
	Alisoles	- 0.21(0.658)	0.41(0.363)	
	Histosol	0.41(0.358)	0(1)	
	Regosol	- 0.51(0.237)	0.2(0.661)	
	Fluviosol	0(1)	0.61(0.144)	
40	*Soil texture	Class		<b>"</b>
ables	A (Sa)	0.85(0.014)	- 0.58(0.175)	iable
oe vari	B (SaLo, LoSa)	- 0.44(0.328)	0.23(0.613)	ic Var
Landscape variables	C (CILo, Lo, SiCILo, Si, SaCILo, SiLo)	-0.39(0.39)	0.45(0.307)	Hydrologic Variables

	Hydrometeorological	Alpha	MTT
	Runoff Coefficient (RC)	0.61(0.144)	0.21(0.645)
	Mean Annual Precipitation (P)	0.11(0.818)	- 0.75(0.052)
	Mean Annual Actual Evapotranspiration (AET)	-0.95(8.1e- 4)	0.39(0.383)
	Mean Annual Streamflow (Q)	0.41(0.355)	- 0.32(0.482)
	Mean Annual Temperature (T)	- 0.54(0.215)	0(1)
	Relative Humidity (RH)	0.34(0.461)	- 0.36(0.427)
	Delta Storage (Δsto)	0.23(0.613)	-0.93(2.5e- 3)
	Seasonal and meteoro	ological Inde	ex
	Seasonality Index (SI)	- 0.63(0.129)	0.68(0.094)
)	Replicability Index (RI)	- 0.16(0.728)	0.57(0.18)



	Topographic	Features		Days Zero Precipitation (Day0)	0.31(0.5)	0.72(0.068)
	Average Slope	0.05(0.908)	- 0.46(0.294)	Variation Coefficient		
	Area - 0.32(0.478) 0.		0.64(0.119)	of daily precipitation (PVAR)	- 0.15(0.756)	0.63(0.129)
	Mean Altitude	0.67(0.10)	- 0.43(0.337)	(1 77.1.4)		
	Dominant Ro	ck types		Months Zero	_	
	Igneous	0.54(0.21)	- 0.67(0.098)	precipitation (Month0)	0.75(0.054)	0.63(0.129)
ogy	Metamorphic	- 0.51(0.237)	-0.2(0.661)	Variation Coefficient of monthly	-	0.54(0.215)
Geology	Sedimentary	- 0.11(0.811)	0.93(2.7e- 3)	precipitation (PMVAR)	0.72(0.068)	0.04(0.210)

<sup>\* (</sup>Sa) sand, (SaLo) Sandy Loam, (LoSa) Loamy Sand, (CILo) Clay loam, (SiCILo) Silty clay loam, (SaCILo) Sandy clay loam, (Lo) Loam, (SiLo) Silty Loam, (Si) Silty. This classification was done according to (Ross et al., 2018). In bold all significant correlations (p-value < 0.1).



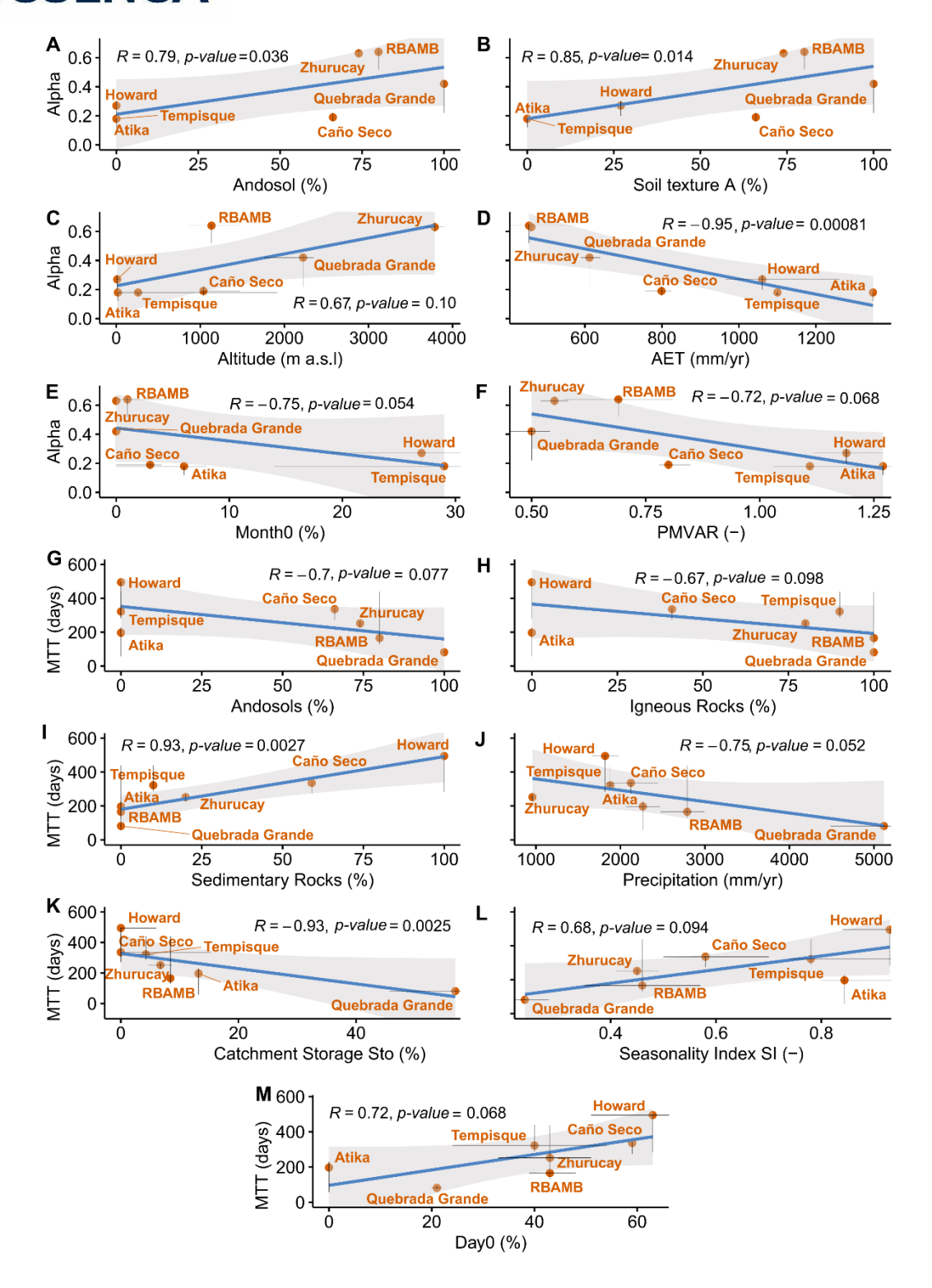


**Figure 4.** Spearman correlations. Alpha parameter ( $\alpha$ ) correlated with: A) percentage of Andosols, B) A group soil texture, C) altitude, D) mean annual evapotranspiration, E) percentage of months with zero precipitation, and F) coefficient of variation with monthly precipitation. MTT values correlated with: G) percentage of Andosols. H) percentage of igneous rock, I) percentage of sedimentary rock, J) mean annual precipitation, K) delta storage (term of the hydrological balance equation  $\Delta$ sto = P-ET-Q), L) seasonality index, and M) percentage of days with zero precipitation. X-axis and y-axis errors are represented with horizontal and vertical lines respectively on each point of the scatter plots.



Furthermore, the %IncMSE of the RF method identified the delta storage and AET as the most important drivers of MTT and the shape of the TT (alpha parameter), respectively (Figure 5). The second most important variables were the sedimentary rocks and the percentage of soil texture A within the catchment. The third most important variables related to MTT and alpha were mean annual precipitation and Andosol soil cover, respectively.

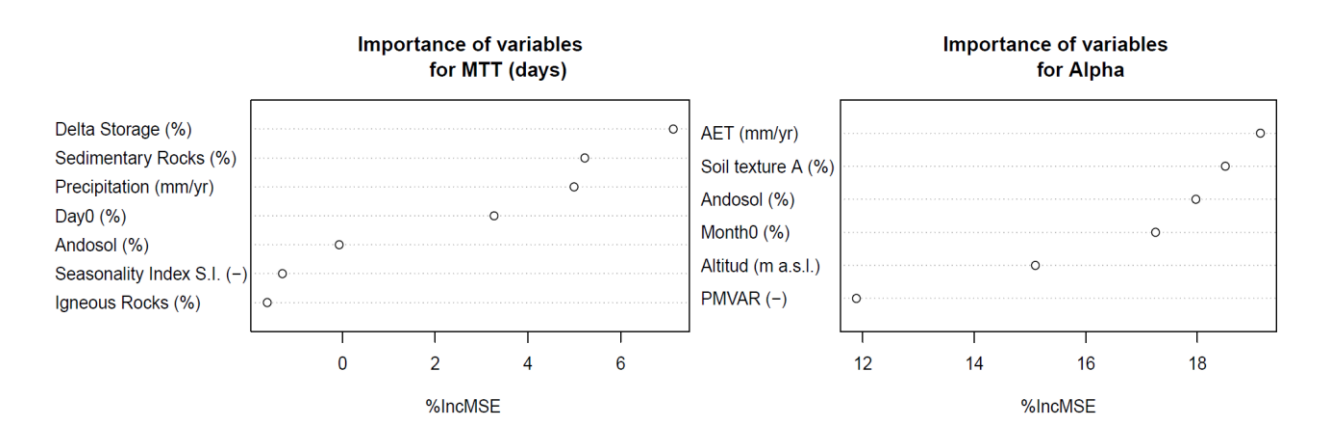


**Figure 5.** Ranking important explanatory variables of MTT and alpha based on the %IncMSE for all predictors used in a Random Forest model.

#### 5. Discussion

#### 5.1. Pan-tropical isotope characteristics and transit time estimates

All the pan-tropical study catchments exhibited relatively similar LMWLs and Evaporation Water Lines (EWL), with a slope close to those of the GMWL (range from 7.7 to 8.35 % and 5.1 to 8.3 %, respectively), indicating limited evaporative fractionation processes (Figure 2). The intercept ranged from 6.5 to 16 ‰, in line with other tropical estimations, where the slope and the intercept values ranged from 6.5 to 9 and from -5 to 25 %, respectively (Putman et al., 2019). In addition to this, d-excess values found in precipitation of the study catchments (8.79 - 14.6), could be associated to non-equilibrium processes such as diffusion across humidity gradients in the tropics indicating evaporation processes for d-excess <10 and humidity recycling for d-excess >10 (Noone, 2012). Similar d-excess values have been previously found in tropical regions such as Costa Rica (8.7 – 13.3 %) (Sánchez-Murillo et al., 2017), and the Amazon rainforest (8 – 17 ‰) (Martinelli et al., 1996). Comparing the variability in precipitation isotopes with the streamflow variability can be indicative of catchment filtering processes most prominent for very damped or averaged out streamflow isotope variability (Tetzlaff et al., 2009). We found variability differences among the catchments but to a lesser degree compared to many other reported studies in the extra-tropics (Figure 2). The latter was reflected in transit time estimates of less than 1.4 years emphasizing the more generally quick response of these hydrological systems. These findings were consistent with previous studies that reported similar transit times but with different methods (Table 3). The gamma model was



able to reflect the dynamics of the isotope signal in streamflow (0.32 > KGE > 0.92), and superior compared with the exponential model (0.16 < KGE < 0.88) (Knoben et al., 2019). Furthermore, the daily sampling frequency particularly of the precipitation input was able to accurately estimate the rapid catchment responses if compared to previous studies that partly reported unidentifiable TTDs using weekly (Hrachowitz, et al., 2009) and bi-weekly (Mosquera et al., 2016; Muñoz-Villers et al., 2016) datasets.

In the Australian Howard catchment, we estimated a best-fit MTT of 494 days (~1.4 years) similar to those reported by Birkel et al. (2020). These longer TTs compared to the other tropical catchments is related to deeper and older groundwater contributing to streamflow as captured by a coupled tracer-aided conceptual rainfall-runoff model that estimated TTs from 1.4 to 3.6 years. In the Atika (Australia), the MTT was 197 days suggesting relatively faster water movement through the Cambisol soils (Lim et al., 2022), which respond quickly to rainfall with a fast infiltration and subsurface stormflow (soil texture class B, Sandy Loam and Loamy Sands) (Bass et al., 2014). Our results are consistent with these previous insights into the fast streamflow response to intense and frequent rainfall events caused by tropical cyclones and monsoon rainfall in the area (Lim et al., 2022).

In Costa Rican catchments, our MTT estimates resulted similar to previous work by Birkel et al. (2016), Correa et al. (2022) and Mayer-Anhalt et al. (2022), all with MTTs of less than one year. Such fast streamflow isotope responses to rainfall resulted from dominant near-surface flow paths with little evidence of deeper and older groundwater even in the larger Tempisque catchment (990km²). Nauditt et al., (2022) reflected on the quick response as a result of limited storage capacity due to the high drought risk in the Tempisque.

Our MTT estimate of ~252 days for the Zhurucay catchment in Ecuador was consistent with previous studies that suggested the prevalence of a "quasi" steady-state with MTTs shorter than 1 year and limited influence from groundwater (Larco et al., 2023; Mosquera et al., 2016; Pesántez et al., 2023).

#### 5.2. Hydrogeomorphic drivers of pan-tropical transit times

We found that the shape of TTDs (alpha parameter) was strongly correlated with soil characteristics and actual evapotranspiration. A similar relationship with soil characteristics was also reported in the much cooler and wet climate of Scotland (Hrachowitz et al., 2009) indicating that soil and storage are primary TT drivers. Furthermore, pan-tropical alpha parameters remained close to and below 0.5, which indicates L-shape distributions with high initial values and a heavy tail (Figure 3). A wide range of North American and European catchments followed this pattern (Godsey et al., 2010; Hrachowitz et al., 2009) suggesting that



more solutes are flushed at short time lags and are present over much longer time scales (Hrachowitz et al., 2010). The latter behavior is directly related to the co-existence of fast nearsurface and slower deeper substrate flow paths, which we can confirm with the most important storage, soil and precipitation variables related to MTTs. For example, Volcanic ash soils (Andosols, r = -0.7, p-value = 0.077) have high water holding capacity (Mosquera et al., 2021) that in combination with low intensity but long frequency precipitation (e.g., Seasonality Index < 0.58) favor relatively quick subsurface flow (Mosquera et al., 2015; Pesántez et al., 2023). Moreover, such soils with macropore flow reduce MTTs (Harman, 2015; Heidbüchel et al., 2020; Mosquera et al., 2020). Consequently, an increase in the percentage cover of these soils will result in shorter MTTs (Figure 3). Therefore, the combination of surface and shallow subsurface preferential flow paths in near-saturated soils above a relatively impermeable bedrock as in the case of the RBAMB and Zhurucay presented relatively higher alpha parameters (0.42 < α < 0.64). On the other hand, catchments such as the Howard, Atika, Caño Seco, and Tempisque, with more freely draining soils, above coarser drift deposits and fractured bedrock resulted in lower alpha parameters ( $\alpha$  < 0.42). The significant correlation of altitude (r = 0.67, p-value = 0.10), actual ET (r = -0.95, p-value = 0.00081) and the alpha parameter suggested that the higher elevation catchments are more energy limited with lower ET compared to lowland catchments. A similar relation to ET and the exposure to energy in form of aspect was previously found by Broxton et al. (2009) in semi-arid catchments in Arizona. Linked to soil characteristics and the capacity of a catchment to conduct or store water were the significant correlations identified by random forest ranked most important controls on TTs and the gamma alpha parameter (Figure 5).

#### 6. Conclusions

Despite the importance of the tropics as a global provider of environmental services, their complex and highly variable dynamics cause a considerable lack of eco-hydrological knowledge. This paper aimed at providing new information for pan-tropical catchments in terms of the hydrogeomorphological influence on transit times. Our analysis revealed potential relationships of TTs with landscape features (soil type), geological variables (igneous, and sedimentary rocks) and hydrological variables (precipitation, storage, seasonality and dry days). These findings suggest that pan-tropical catchments are more connected to subsurface processes and storage than it was previously thought.

TTs of pan-tropical catchments are shorter than 1.4 years indicating the expected relatively fast and dynamic flows and material transport. The gamma model estimated TTDs showed that more solutes are flushed at shorter time scales in contrast with the almost globally valid TTD of  $\alpha = 0.5$ . Our analysis revealed statistically significant correlations (0.67 < r < 0.85, p-



value < 0.1) associated with landscape features (storage capacity, soil characteristics and mean altitude), and (-0.95 < r < -0.72, p-value < 0.068) hydrologic variables (months with zero precipitation, precipitation, the coefficient of variation of monthly precipitation and actual evapotranspiration). Despite the stationary TTs used in this study, our findings provided more details about how physical variables influence the hydrological flow pathways of the tropics, which is essential for an appropriate water resources management and climate change adaptation strategies in tropical catchments.



#### References

- Amin, I. E., & Campana, M. E. (1996). A general lumped parameter model for the interpretation of tracer data and transit time calculation in hydrologic systems. *Journal of Hydrology*, 179(1–4), 1–21. https://doi.org/10.1016/0022-1694(95)02880-3
- Arciniega-Esparza, S., Birkel, C., Durán-Quesada, A. M., Sánchez-Murillo, R., Moore, G. W., Maneta, M. P., Boll, J., Negri, L. B., Tetzlaff, D., Yoshimura, K., & Soulsby, C. (2023). Tracer-aided ecohydrological modelling across climate, land cover, and topographical gradients in the tropics. *Hydrological Processes*, 37(5), e14884. https://doi.org/10.1002/hyp.14884
- Ardia, D., Boudt, K., Carl, P., Mullen, K. M., & Peterson, B. G. (2011). Differential Evolution with DEoptim

  An Application to Non-Convex Portfolio Optimiza-tion. *The R Journal*, 2–34.

  https://doi.org/10.32614/RJ-2011-005
- Barlow, J., França, F., Gardner, T. A., Hicks, C. C., Lennox, G. D., Berenguer, E., Castello, L., Economo,
  E. P., Ferreira, J., Guénard, B., Gontijo Leal, C., Isaac, V., Lees, A. C., Parr, C. L., Wilson, S.
  K., Young, P. J., & Graham, N. A. J. (2018). The future of hyperdiverse tropical ecosystems.
  Nature, 559(7715), 517–526. https://doi.org/10.1038/s41586-018-0301-1
- Bass, A. M., Munksgaard, N. C., Leblanc, M., Tweed, S., & Bird, M. I. (2014). Contrasting carbon export dynamics of human impacted and pristine tropical catchments in response to a short-lived discharge event: TROPICAL FLUVIAL CARBON EXPORT. *Hydrological Processes*, 28(4), 1835–1843. https://doi.org/10.1002/hyp.9716
- Beck, H. E., Zimmermann, N. E., Mcvicar, T. R., Vergopolan, N., Berg, A., & Wood, E. F. (2018). *Data Descriptor: Present and future Köppen-Geiger climate classification maps at 1-km resolution*. https://doi.org/10.1038/sdata.2018.214
- Benettin, P., Rodriguez, N. B., Sprenger, M., Kim, M., Klaus, J., Harman, C. J., van der Velde, Y., Hrachowitz, M., Botter, G., McGuire, K. J., Kirchner, J. W., Rinaldo, A., & McDonnell, J. J. (2022). Transit Time Estimation in Catchments: Recent Developments and Future Directions.

  \*Water Resources Research, 58(11), e2022WR033096.

  https://doi.org/10.1029/2022WR033096
- Benettin, P., Soulsby, C., Birkel, C., Tetzlaff, D., Botter, G., & Rinaldo, A. (2017). Using SAS functions and high-resolution isotope data to unravel travel time distributions in headwater catchments.

  Water Resources Research, 53(3), 1864–1878. https://doi.org/10.1002/2016WR020117



- Bergoeing, J. (2007). Geomorfologia de Costa Rica.
- Beven, K. J. (2010). Preferential flows and travel time distributions: Defining adequate hypothesis tests for hydrological process models. *Hydrological Processes*, *24*(12), 1537–1547. https://doi.org/10.1002/hyp.7718
- Birkel, C., Correa Barahona, A., Duvert, C., Granados Bolaños, S., Chavarría Palma, A., Durán Quesada, A. M., Sánchez Murillo, R., & Biester, H. (2021). End member and Bayesian mixing models consistently indicate near-surface flowpath dominance in a pristine humid tropical rainforest. *Hydrological Processes*, *35*(4). https://doi.org/10.1002/hyp.14153
- Birkel, C., Duvert, C., Correa, A., Munksgaard, N. C., Maher, D. T., & Hutley, L. B. (2020). Tracer-Aided Modeling in the Low-Relief, Wet-Dry Tropics Suggests Water Ages and DOC Export Are Driven by Seasonal Wetlands and Deep Groundwater. *Water Resources Research*, *56*(4), e2019WR026175. https://doi.org/10.1029/2019WR026175
- Birkel, C., Geris, J., Molina, M. J., Mendez, C., Arce, R., Dick, J., Tetzlaff, D., & Soulsby, C. (2016).

  Hydroclimatic controls on non-stationary stream water ages in humid tropical catchments. *Journal of Hydrology*, *542*, 231–240. https://doi.org/10.1016/j.jhydrol.2016.09.006
- Birkel, C., & Soulsby, C. (2015). Advancing tracer-aided rainfall-runoff modelling: A review of progress, problems and unrealised potential. *Hydrological Processes*, 29(25), 5227–5240. https://doi.org/10.1002/hyp.10594
- Blewett, R. (2012). Shaping a Nation: A Geology of Australia.
- Blöschl, G., Bierkens, M. F. P., Chambel, A., Cudennec, C., Destouni, G., Fiori, A., Kirchner, J. W., McDonnell, J. J., Savenije, H. H. G., Sivapalan, M., Yilmaz, K. K., & Zhang, Y. (2019). Twenty-three unsolved problems in hydrology (UPH)—a community perspective. *Hydrological Sciences Journal*, *64*(10), 1141–1158. https://doi.org/10.1080/02626667.2019.1620507
- Breiman, L. (2001). Random Forests. *Machine Learning*, *45*(1), 5–32. https://doi.org/10.1023/A:1010933404324.
- Brocklehurst, P. (2012). Soils of the Northern Territory factsheet [Government]. Northern Territory Government. https://depws.nt.gov.au/rangelands/technical-notes-and-fact-sheets/land-soil-vegetation-technical-information



- Broxton, P. D., Troch, P. A., & Lyon, S. W. (2009). On the role of aspect to quantify water transit times in small mountainous catchments. *Water Resources Research*, *45*(8). https://doi.org/10.1029/2008WR007438
- Cai, W., Wu, L., Lengaigne, M., Li, T., McGregor, S., Kug, J.-S., Yu, J.-Y., Stuecker, M. F., Santoso, A., Li, X., Ham, Y.-G., Chikamoto, Y., Ng, B., McPhaden, M. J., Du, Y., Dommenget, D., Jia, F., Kajtar, J. B., Keenlyside, N., ... Chang, P. (2019). Pantropical climate interactions. *Science*, 363(6430), eaav4236. https://doi.org/10.1126/science.aav4236
- Cartwright, I., Morgenstern, U., Howcroft, W., Hofmann, H., Armit, R., Stewart, M., Burton, C., & Irvine, D. (2020). The variation and controls of mean transit times in Australian headwater catchments. *Hydrological Processes*, *34*(21), 4034–4048. https://doi.org/10.1002/hyp.13862
- Coltorti, M., & Ollier, C. D. (2000). Geomorphic and tectonic evolution of the Ecuadorian Andes. *Geomorphology*, 32(1), 1–19. https://doi.org/10.1016/S0169-555X(99)00036-7
- Cook, Hatton, T. J., Pidsley, D., Herczeg, A. L., Held, A., O'Grady, A., & Eamus, D. (1998). Water balance of a tropical woodland ecosystem, Northern Australia: A combination of micrometeorological, soil physical and groundwater chemical approaches. *Journal of Hydrology*, 210(1–4), 161–177. https://doi.org/10.1016/S0022-1694(98)00181-4
- Cook, R. D., & Weisberg, S. (1983). Diagnostics for Heteroscedasticity in Regression. *Biometrika*, 70(1), 1–10. https://doi.org/10.2307/2335938
- Correa, A., Birkel, C., Gutierrez, J., Dehaspe, J., Durán-Quesada, A. M., Soulsby, C., & Sánchez-Murillo, R. (2020). Modelling non-stationary water ages in a tropical rainforest: A preliminary spatially distributed assessment. *Hydrological Processes*, *34*(25), 4776–4793. https://doi.org/10.1002/hyp.13925
- Dehaspe, J., Birkel, C., Tetzlaff, D., Sánchez-Murillo, R., Durán-Quesada, A. M., & Soulsby, C. (2018).

  Spatially distributed tracer-aided modelling to explore water and isotope transport, storage and mixing in a pristine, humid tropical catchment. *Hydrological Processes*. https://doi.org/10.1002/hyp.13258
- Denyer, P., & Kussmaul, S. (Eds.). (2000). *Geología de Costa Rica* (1. ed). Editorial Tecnológica de Costa Rica.
- Doyle, N. (2001). Extractive minerals within the outer Darwin area. Gov. Printer of the Northern Territory.



- Driessen, P. M. (Ed.). (2001). *Lecture notes on the major soils of the world*. Food and Agriculture Organization of the United Nations- FAO.
- Duvert, C., Hutley, L. B., Birkel, C., Rudge, M., Munksgaard, N. C., Wynn, J. G., Setterfield, S. A., Cendón, D. I., & Bird, M. I. (2020). Seasonal Shift From Biogenic to Geogenic Fluvial Carbon Caused by Changing Water Sources in the Wet-Dry Tropics. *Journal of Geophysical Research: Biogeosciences*, 125(2). https://doi.org/10.1029/2019JG005384
- Duvert, C., Lim, H.-S., Irvine, D. J., Bird, M. I., Bass, A. M., Tweed, S. O., Hutley, L. B., & Munksgaard, N. C. (2022). Hydrological processes in tropical Australia: Historical perspective and the need for a catchment observatory network to address future development. *Journal of Hydrology: Regional Studies*, 43, 101194. https://doi.org/10.1016/j.ejrh.2022.101194
- Erlich, R. N., Astorga, A., Sofer, Z., Pratt, L. M., & Palmer, S. E. (1996). Palaeoceanography of organic-rich rocks of the Loma Chumico Formation of Costa Rica, Late Cretaceous, eastern Pacific. Sedimentology, 43(4), 691–718. https://doi.org/10.1111/j.1365-3091.1996.tb02021.x
- Gastwirth, J. L., Gel, Y. R., Hui, W. L. W., Lyubchich, V., Miao, W., & Noguchi, K. (2023). *lawstat: Tools for Biostatistics, Public Policy, and Law* (3.6). https://cran.r-project.org/web/packages/lawstat/index.html
- Godsey, S. E., Aas, W., Clair, T. A., de Wit, H. A., Fernandez, I. J., Kahl, J. S., Malcolm, I. A., Neal, C., Neal, M., Nelson, S. J., Norton, S. A., Palucis, M. C., Skjelkvåle, B. L., Soulsby, C., Tetzlaff, D., & Kirchner, J. W. (2010). Generality of fractal 1/f scaling in catchment tracer time series, and its implications for catchment travel time distributions. *Hydrological Processes*, 24(12), 1660–1671. https://doi.org/10.1002/hyp.7677
- Gröning, M., Lutz, H. O., Roller-Lutz, Z., Kralik, M., Gourcy, L., & Pöltenstein, L. (2012). A simple rain collector preventing water re-evaporation dedicated for δ18O and δ2H analysis of cumulative precipitation samples. *Journal of Hydrology*, 448–449, 195–200. https://doi.org/10.1016/j.jhydrol.2012.04.041
- Gupta, H. V., Kling, H., Yilmaz, K. K., & Martinez, G. F. (2009). Decomposition of the mean squared error and NSE performance criteria: Implications for improving hydrological modelling. *Journal of Hydrology*, 377(1–2), 80–91. https://doi.org/10.1016/J.JHYDROL.2009.08.003
- Guzman, I., & Calvo, J. (2013). Planning and development of Costa Rica water resources: Current status and perspectives.



- Harman, C. J. (2015). Time-variable transit time distributions and transport: Theory and application to storage-dependent transport of chloride in a watershed. *Water Resources Research*, *51*(1), 1–30. https://doi.org/10.1002/2014WR015707
- Heidbüchel, I., Yang, J., Musolff, A., Troch, P., Ferré, T., & Fleckenstein, J. H. (2020). On the shape of forward transit time distributions in low-order catchments. *Hydrology and Earth System Sciences*, *24*(6), 2895–2920. https://doi.org/10.5194/hess-24-2895-2020
- Hrachowitz, M., Savenije, H., Bogaard, T. A., Tetzlaff, D., & Soulsby, C. (2013). What can flux tracking teach us about water age distribution patterns and their temporal dynamics? *Hydrology and Earth System Sciences*, *17*(2), 533–564. https://doi.org/10.5194/hess-17-533-2013
- Hrachowitz, M., Soulsby, C., Tetzlaff, D., Dawson, J. J. C., Dunn, S. M., & Malcolm, I. A. (2009). Using long-term data sets to understand transit times in contrasting headwater catchments. *Journal of Hydrology*, 367(3–4), 237–248. https://doi.org/10.1016/J.JHYDROL.2009.01.001
- Hrachowitz, M., Soulsby, C., Tetzlaff, D., Dawson, J. J. C., & Malcolm, I. A. (2009). Regionalization of transit time estimates in montane catchments by integrating landscape controls. *Water Resources Research*, *45*(5). https://doi.org/10.1029/2008WR007496
- Hrachowitz, M., Soulsby, C., Tetzlaff, D., Malcolm, I. A., & Schoups, G. (2010). Gamma distribution models for transit time estimation in catchments: Physical interpretation of parameters and implications for time-variant transit time assessment. Water Resources Research, 46(10). https://doi.org/10.1029/2010WR009148
- Jacobs, S. R., Timbe, E., Weeser, B., Rufino, M. C., Butterbach-Bahl, K., & Breuer, L. (2018).

  Assessment of hydrological pathways in East African montane catchments under different land use. *Hydrol. Earth Syst. Sci*, 22, 4981–5000. https://doi.org/10.5194/hess-22-4981-2018
- Kannan, M., López, C., Jacobsen, D., & Guerra, M. (2020). History of limnology in Ecuador: A foundation for a growing field in the country. *Hydrobiologia*, 847. https://doi.org/10.1007/s10750-020-04291-1
- King, A. P., & Eckersley, R. J. (2019). Chapter 7 Inferential Statistics IV: Choosing a Hypothesis Test.
  In A. P. King & R. J. Eckersley (Eds.), Statistics for Biomedical Engineers and Scientists (pp. 147–171). Academic Press. https://doi.org/10.1016/B978-0-08-102939-8.00016-5
- Kirchner, J. W. (2016). Aggregation in environmental systems Part 1: Seasonal tracer cycles quantify young water fractions, but not mean transit times, in spatially heterogeneous



- catchments. *Hydrology and Earth System Sciences*, 20(1), 279–297. https://doi.org/10.5194/hess-20-279-2016
- Klaus, J., Chun, K. P., McGuire, K. J., & McDonnell, J. J. (2015). Temporal dynamics of catchment transit times from stable isotope data. *Water Resources Research*, *51*(6), 4208–4223. https://doi.org/10.1002/2014WR016247
- Knapp, J. L. A., Neal, C., Schlumpf, A., Neal, M., & Kirchner, J. W. (2019). New water fractions and transit time distributions at Plynlimon, Wales, estimated from stable water isotopes in precipitation and streamflow. *Hydrology and Earth System Sciences*, 23(10), 4367–4388. https://doi.org/10.5194/hess-23-4367-2019
- Knoben, W., Freer, J., & Woods, R. (2019). Technical note: Inherent benchmark or not? Comparing Nash-Sutcliffe and Kling-Gupta efficiency scores. *Hydrology and Earth System Sciences Discussions*, 1–7. https://doi.org/10.5194/hess-2019-327
- Köppen, W. (1936). Das geographische System der Klimate (1936). 44.
- Krasilnikov, P., Marti, J.-J. I., Arnold, R., & Shoba, S. (Eds.). (2009). *A Handbook of Soil Terminology, Correlation and Classification* (0 ed.). Routledge. https://doi.org/10.4324/9781849774352
- Land and Water Division. (2006). *Guidelines for soil description*. FAO. https://www.fao.org/publications/card/en/c/903943c7-f56a-521a-8d32-459e7e0cdae9/
- Larco, K., Mosquera, G. M., Jacobs, S. R., Cardenas, I., & Crespo, P. (2023). Factors controlling the temporal variability of streamflow transit times in tropical alpine catchments. *Journal of Hydrology*, *617*, 128990. https://doi.org/10.1016/j.jhydrol.2022.128990
- Liaw, A., & Wiener, M. (2001). Classification and Regression by RandomForest. Forest, 23.
- Lim, H. S., Munksgaard, N. C., & Bird, M. I. (2022). Revisiting Michael Bonell's work on humid tropical rainforest catchments: Isotope tracers reveal seasonal shifts in catchment hydrology.

  Hydrological Processes, 36(10). https://doi.org/10.1002/hyp.14722
- Longo, R., & Baldock, J. (1982). *National Geological Map of the Republic of Ecuador (including Galápagos Province)*. [Research]. EUROPEAN SOIL DATA CENTRE (ESDAC). https://esdac.jrc.ec.europa.eu/images/Eudasm/latinamerica/images/maps/download/ec12005
  \_ge.jpg



- Macdonald, F. A., Swanson-Hysell, N. L., Park, Y., Lisiecki, L., & Jagoutz, O. (2019). Arc-continent collisions in the tropics set Earth's climate state. *Science*, *364*(6436), 181–184. https://doi.org/10.1126/science.aav5300
- Małoszewski, P., & Zuber, A. (1982). Determining the turnover time of groundwater systems with the aid of environmental tracers: 1. Models and their applicability. *Journal of Hydrology*, *57*(3–4), 207–231. https://doi.org/10.1016/0022-1694(82)90147-0
- Martinelli, L. A., Victoria, R. L., Silveira Lobo Sternberg, L., Ribeiro, A., & Zacharias Moreira, M. (1996).

  Using stable isotopes to determine sources of evaporated water to the atmosphere in the Amazon basin. *Journal of Hydrology*, 183(3), 191–204. https://doi.org/10.1016/0022-1694(95)02974-5
- Martínez-Cuenca, M.-R., Pereira-Dias, L., Soler, S., López-Serrano, L., Alonso, D., Calatayud, Á., & Díez, M. J. (2020). Adaptation to Water and Salt Stresses of Solanum pimpinellifolium and Solanum lycopersicum var. Cerasiforme. *Agronomy*, *10*(8), 1169. https://doi.org/10.3390/agronomy10081169
- Mayer-Anhalt, L., Birkel, C., Sánchez-Murillo, R., & Schulz, S. (2022). Tracer-aided modelling reveals quick runoff generation and young streamflow ages in a tropical rainforest catchment. *Hydrological Processes*, 36(2). https://doi.org/10.1002/hyp.14508
- McDonnell, J. J., McGuire, K., Aggarwal, P., Beven, K. J., Biondi, D., Destouni, G., Dunn, S., James,
  A., Kirchner, J., Kraft, P., Lyon, S., Maloszewski, P., Newman, B., Pfister, L., Rinaldo, A.,
  Rodhe, A., Sayama, T., Seibert, J., Solomon, K., ... Wrede, S. (2010). How old is streamwater?
  Open questions in catchment transit time conceptualization, modelling and analysis.
  Hydrological Processes, 24(12), 1745–1754. https://doi.org/10.1002/hyp.7796
- McGuire, K. J., & McDonnell, J. J. (2006). A review and evaluation of catchment transit time modeling. *Journal of Hydrology*, 330(3–4), 543–563. https://doi.org/10.1016/j.jhydrol.2006.04.020
- McGuire, K. J., McDonnell, J. J., Weiler, M., Kendall, C., McGlynn, B. L., Welker, J. M., & Seibert, J. (2005). The role of topography on catchment-scale water residence time. *Water Resources Research*, *41*(5). https://doi.org/10.1029/2004WR003657
- Mosquera, G. M., Crespo, P., Breuer, L., Feyen, J., & Windhorst, D. (2020). Water transport and tracer mixing in volcanic ash soils at a tropical hillslope: A wet layered sloping sponge. *Hydrological Processes*, *34*(9), 2032–2047. https://doi.org/10.1002/hyp.13733



- Mosquera, G. M., Franklin, M., Jan, F., Rolando, C., Lutz, B., David, W., & Patricio, C. (2021). A field, laboratory, and literature review evaluation of the water retention curve of volcanic ash soils:

  How well do standard laboratory methods reflect field conditions? *Hydrological Processes*, 35(1). https://doi.org/10.1002/hyp.14011
- Mosquera, G. M., Lazo, P. X., Célleri, R., Wilcox, B. P., & Crespo, P. (2015). Runoff from tropical alpine grasslands increases with areal extent of wetlands. *CATENA*, *125*, 120–128. https://doi.org/10.1016/j.catena.2014.10.010
- Mosquera, G. M., Segura, C., Vaché, K. B., Windhorst, D., Breuer, L., & Crespo, P. (2016). Insights into the water mean transit time in a high-elevation tropical ecosystem. *Hydrology and Earth System Sciences*, *20*(7), 2987–3004. https://doi.org/10.5194/hess-20-2987-2016
- Moya Arguedas, M. (1990). Diagnóstico para el control de inundaciones y ordenamiento de la Cuenca del Río Corredores, Región Brunca, Costa Rica /. Vicerrectoría de Investigacion, Departamento de Geografia,.
- Muñoz-Villers, L. E., Geissert, D. R., Holwerda, F., & McDonnell, J. J. (2016). Factors influencing stream baseflow transit times in tropical montane watersheds. *Hydrology and Earth System Sciences*, 20(4), 1621–1635. https://doi.org/10.5194/hess-20-1621-2016
- Murtha, G. G. (1986). Soils of the Tully-Innisfail Area, North Queensland. Townsville, QLD, CSIRO Divison of Soils. https://doi.org/10.4225/08/585ac669675d7
- Nauditt, A., Stahl, K., Rodríguez, E., Birkel, C., Formiga-Johnsson, R. M., Kallio, M., Ribbe, L., Baez-Villanueva, O. M., Thurner, J., & Hann, H. (2022). Evaluating tropical drought risk by combining open access gridded vulnerability and hazard data products. *Science of The Total Environment*, 822, 153493. https://doi.org/10.1016/j.scitotenv.2022.153493
- Noone, D. (2012). Pairing Measurements of the Water Vapor Isotope Ratio with Humidity to Deduce Atmospheric Moistening and Dehydration in the Tropical Midtroposphere. *Journal of Climate*, 25(13), 4476–4494. https://doi.org/10.1175/JCLI-D-11-00582.1
- Osborne, J. W., & Waters, E. (2002). Four assumptions of multiple regression that researchers should always test. https://doi.org/10.7275/R222-HV23
- Pedhazur, E. J. (1997). *Multiple regression in behavioral research: Explanation and prediction* (3rd ed). Harcourt Brace College Publishers.



- Peel, M. C., Finlayson, B. L., & McMahon, T. A. (2007). Updated world map of the Köppen-Geiger climate classification. *Hydrology and Earth System Sciences*, 11(5), 1633–1644. https://doi.org/10.5194/hess-11-1633-2007
- Peña, E. A., & Slate, E. H. (2006). Global Validation of Linear Model Assumptions. *Journal of the American Statistical Association*, 101(473), 341–354. https://doi.org/10.1198/016214505000000637
- Pesántez, J., Birkel, C., Mosquera, G. M., Célleri, R., Contreras, P., Cárdenas, I., & Crespo, P. (2023).

  Bridging the gap from hydrological to biogeochemical processes using tracer-aided hydrological models in a tropical montane ecosystem. *Journal of Hydrology*, *619*, 129328. https://doi.org/10.1016/j.jhydrol.2023.129328
- Pratt, W. T., Figueroa, J., & Flores, B. (Eds.). (1997). *Geology of the Cordillera Occidental of Ecuador between* 3°00' and 4°00'S. Quito.
- Putman, A. L., Fiorella, R. P., Bowen, G. J., & Cai, Z. (2019). A Global Perspective on Local Meteoric Water Lines: Meta-analytic Insight Into Fundamental Controls and Practical Constraints. *Water Resources Research*, *55*(8), 6896–6910. https://doi.org/10.1029/2019WR025181
- Quichimbo, P., Tenorio, G., Borja, P., Cárdenas, I., Crespo, P., & Célleri, R. (2012). EFECTOS SOBRE LAS PROPIEDADES FÍSICAS Y QUÍMICAS DE LOS SUELOS POR EL CAMBIO DE LA COBERTURA VEGETAL Y USO DEL SUELO: PÁRAMO DE QUIMSACOCHA AL SUR DEL ECUADOR. Suelos Ecuatoriales, 42, 138–156.
- R Core Team. (2021). R: A language and environment for statistical computing. R Foundation for statistical Computing, Vienna, Austria. https://www.R-project.org/.
- Rinaldo, A., Beven, K. J., Bertuzzo, E., Nicotina, L., Davies, J., Fiori, A., Russo, D., & Botter, G. (2011).

  Catchment travel time distributions and water flow in soils. *Water Resources Research*, *47*(7).

  https://doi.org/10.1029/2011WR010478
- Ross, C. W., Prihodko, L., Anchang, J., Kumar, S., Ji, W., & Hanan, N. P. (2018). HYSOGs250m, global gridded hydrologic soil groups for curve-number-based runoff modeling. *Scientific Data*, *5*(1), 180091. https://doi.org/10.1038/sdata.2018.91
- Sánchez-Murillo, R., Durán-Quesada, A. M., Birkel, C., Esquivel-Hernández, G., & Boll, J. (2017).

  Tropical precipitation anomalies and *d*-excess evolution during El Niño 2014-16. *Hydrological Processes*, *31*(4), 956–967. https://doi.org/10.1002/hyp.11088



- Sánchez-Murillo, R., Romero-Esquivel, L. G., Jiménez-Antillón, J., Salas-Navarro, J., Corrales-Salazar,
  L., Álvarez-Carvajal, J., Álvarez-McInerney, S., Bonilla-Barrantes, D., Gutiérrez-Sibaja, N.,
  Martínez-Arroyo, M., Ortiz-Apuy, E., Salgado-Lobo, J., Villalobos-Morales, J., Esquivel-Hernández, G., Rojas-Jiménez, L. D., Gómez-Castro, C., Jiménez-Madrigal, Q., Vargas-Gutiérrez, O., & Birkel, C. (2019). DOC Transport and Export in a Dynamic Tropical Catchment.
  Journal of Geophysical Research: Biogeosciences, 124(6), 1665–1679.
  https://doi.org/10.1029/2018JG004897
- Savin, N. E., & White, K. J. (1977). The Durbin-Watson Test for Serial Correlation with Extreme Sample Sizes or Many Regressors. *Econometrica*, 45(8), 1989–1996. https://doi.org/10.2307/1914122 Singh, V. P. (1991). *Elementary Hydrology*.
- Soulsby, C., Birkel, C., & Tetzlaff, D. (2014). Assessing urbanization impacts on catchment transit times. *Geophysical Research Letters*, *41*(2), 442–448. https://doi.org/10.1002/2013GL058716
- Stewart, M. K., & McDonnell, J. J. (1991). Modeling Base Flow Soil Water Residence Times From Deuterium Concentrations. *Water Resources Research*, 27(10), 2681–2693. https://doi.org/10.1029/91WR01569
- Stewart, M. K., Morgenstern, U., & McDonnell, J. J. (2010). Truncation of stream residence time: How the use of stable isotopes has skewed our concept of streamwater age and origin. *Hydrological Processes*, *24*(12), 1646–1659. https://doi.org/10.1002/hyp.7576
- Tetzlaff, D., Seibert, J., McGuire, K. J., Laudon, H., Burns, D. A., Dunn, S. M., & Soulsby, C. (2009).

  How does landscape structure influence catchment transit time across different geomorphic provinces? *Hydrological Processes*, 23(6), 945–953. https://doi.org/10.1002/hyp.7240
- Timbe, E., Windhorst, D., Crespo, P., Frede, H.-G., Feyen, J., & Breuer, L. (2014). Understanding uncertainties when inferring mean transit times of water trough tracer-based lumped-parameter models in Andean tropical montane cloud forest catchments. *Hydrology and Earth System Sciences*, 18(4), 1503–1523. https://doi.org/10.5194/hess-18-1503-2014
- Venegas-Cordero, N., Birkel, C., Giraldo-Osorio, J. D., Correa-Barahona, A., Duran-Quesada, A. M., Arce-Mesen, R., & Nauditt, A. (2021). Can hydrological drought be efficiently predicted by conceptual rainfall-runoff models with global data products? *Journal of Natural Resources and Development*, 20-37 Pages. https://doi.org/10.18716/OJS/JNRD/2021.11.01



- Walsh, R. P. D., & Lawler, D. M. (1981). Rainfall Seasonality: Description, Spatial Patterns and Change Through Time. *Weather*, *36*(7), 201–208. https://doi.org/10.1002/j.1477-8696.1981.tb05400.x
- Williams, M. N., Grajales, C. A. G., & Kurkiewicz, D. (2013). *Assumptions of Multiple Regression:*Correcting Two Misconceptions. https://doi.org/10.7275/55HN-WK47
- Wissler, C. (1905). The Spearman Correlation Formula. *Science*, *22*(558), 309–311. https://doi.org/10.1126/science.22.558.309
- Wohl, E., Barros, A., Brunsell, N., Chappell, N. A., Coe, M., Giambelluca, T., Goldsmith, S., Harmon, R., Hendrickx, J. M. H., Juvik, J., McDonnell, J., & Ogden, F. (2012). The hydrology of the humid tropics. *Nature Climate Change*, 2(9), 655–662. https://doi.org/10.1038/nclimate1556



#### **Annexes**

#### Annex A. Data source and descriptive statistics of isotopic signatures

Statistical descriptions (i.e., n-number of observations,  $\bar{x}$ -media,  $\tilde{x}$ -median, sd- standard deviations, [min, max] range) of isotopic concentration in precipitation and streamflow of two conservative tracers: deuterium ( $\delta^2$ H) and oxygen-18 ( $\delta^{18}$ O). Samples were collected on daily time scale from the current catchments, which are constantly monitored by Costa Rica University-Costa Rica, James Cook University- Australia and University of Cuenca-Ecuador in cooperation with the IAEA. Data from RBAMB and Zhurucay catchments are available at an intra-hourly scale and were aggregated to daily scale for a standard daily treatment of the entire pan-tropical dataset of catchments.

**Table A.** Data source and descriptive statistics of isotopic signatures: Deuterium (<sup>2</sup>H) and Oxygen-18 (<sup>18</sup>O) were measured.

Catchment s			Howard	Atika	Caño Seco	Quebra da Grande	RBAMB	Tempisque	Zhurucay
Equipment		*CRDSL Picarro L2130-i	*CRDSL Picarro 2130-i	**DLT- 100 Los Gatos	*CRDS Picarro L2120-i	*CRDS Picarro L2120-i	*CRDS Picarro L2120-i	*CRDS Picarro L2130-i	
		n	370	309	555	914	2024	484	4310
	_	$ar{x}$ $ ilde{x}$	-29.6 -26.33	-7.98 2.44	-57.96 -62.05	-26.76 -20.64	-26.56 -28.52	-38.1 -36.2	-72.85 -65.90
_	δ²H	sd	26.6	24.96	22.97	33.3	11.02	24.36	35.55
Precipitation		[Min; max]	[-111.4; 22.56]	[-15.13; 30.93]	[- 135.91; -1.46]	[- 161.04, 21.23]	[-65.84; 21.22]	[-111.85; 12.28]	[-184.96; 0.01]
eC.		n	370	309	234	914	102	484	4310
Ţ		$\bar{x}$	-5.5	-2.81	-8.52	-5	-5.16	-5.88	-10.02
	8180	$\widetilde{x}$	-5.34	-1.55	-9.16	-4.1	-4.65	-5.72	-9.38
	Ø	sd	3.43	3.09	2.87	3.99	2.8	3.16	4.40
		[Min;	[-15.8;	[-15.26;	[-18.17;	[-21.06;	[-8.88;	[-15.29;	[-24.98;
		max]	0.29]	2.88]	-0.89]	0.69]	-3.80]	1.16]	-2.43]
		n	47	163	247	395	223	171	3918
		$\bar{x}$	-32.7	-26.52	-63.00	-30.34	-26.21	-40.31	-73.04
	8 <sup>2</sup> H	$\tilde{x}$	-31.08	-26.33	-64.17	-34.46	-26.06	-39.24	-71.72
>	Ю	sd	5.82	11.83	4.47	13.70	3.32	4.91	7.27
Ę.		[Min;	[-58.94;	[-53.28;	[-79.37;	[-79.23,	[-40.69;	[-72.60;	[-108.63;
Streamflow		max]	-26.45] 47	5.27] 163	-21.88] 234	-1.39] 395	-15.79] 200	-34.08] 171	-54.66] 3958
ě		n <del>«</del>	-5.33	-5.32	-9.30	-5.55	-5.02	-6.48	-10.58
S	0	$ar{x}$ $ ilde{x}$	-5.33 -5.09	-5.32 -5.23	-9.30 -9.46	-5.56	-5.02 -5.02	-6.38	-10.36 -10.42
	8180	x sd	-5.09 1.04	-5.23 1.54	-9. <del>4</del> 6 0.58	-5.56 1.58	-5.02 0.52	-0.36 0.77	-10. <del>4</del> 2 0.95
	Ю	[Min;	1.0 <del>4</del> [-9.5;	[-8.82;	[-11.49;	[-12.04;	0.32 [-7.26;	[-10.23;	[-15.29;
		max]	[-9.5, -4.01]	-0.02, -1.37]	-1.27]	[-12.0 <del>4</del> , -2.29]	-3.63]	-5.32]	-6.26]

<sup>\*</sup>Standard errors reported by the analysis  $\pm\sigma$ :  $\pm0.5$  % for  $\delta^2H$  and  $\pm0.1$  % for  $\delta^1BO$ . \*\*  $\pm\sigma$ :  $\pm0.4$  % for  $\delta^2H$  and  $\pm0.1$  % for  $\delta^1BO$ . Tracer metrics used for comparison between catchments.  $\bar{x}$  media,  $\tilde{x}$  median, n number of observations, sd standard deviation.



Annex B. Data records of all catchments

Table B. Available data records of all catchments.

Study catchments	Dataset	Warming-up period	Calibration Period
Howard	May-2015 /May 2018	Dec-2016 /April 2017	May-2015 /May 2018
Atika	Jan-2019/Oct 2021	Nov-2020/April 2021	Jan-2019/Jul- 2021
Caño Seco	Jan-2012/Sep-2014	Jun-2013/Nov- 2013	May-2012/May-2014
Quebrada Grande	Jan-2016/Dec-2019	0ct-2015/April-2017	Jan-2016/Dec-2019
RBAMB	Jan-2013/Jul-2018	March-2017/Sep- 017	Jan-2015/Jul-2018
Tempisque	Jun-2015/Aug 2021	Jul-2020/April-2021	Jun-2015/Aug 2021
Zhurucay	Oct-2017/Feb-2019	May-2018/Feb 2019	Oct-2017/Feb-2019

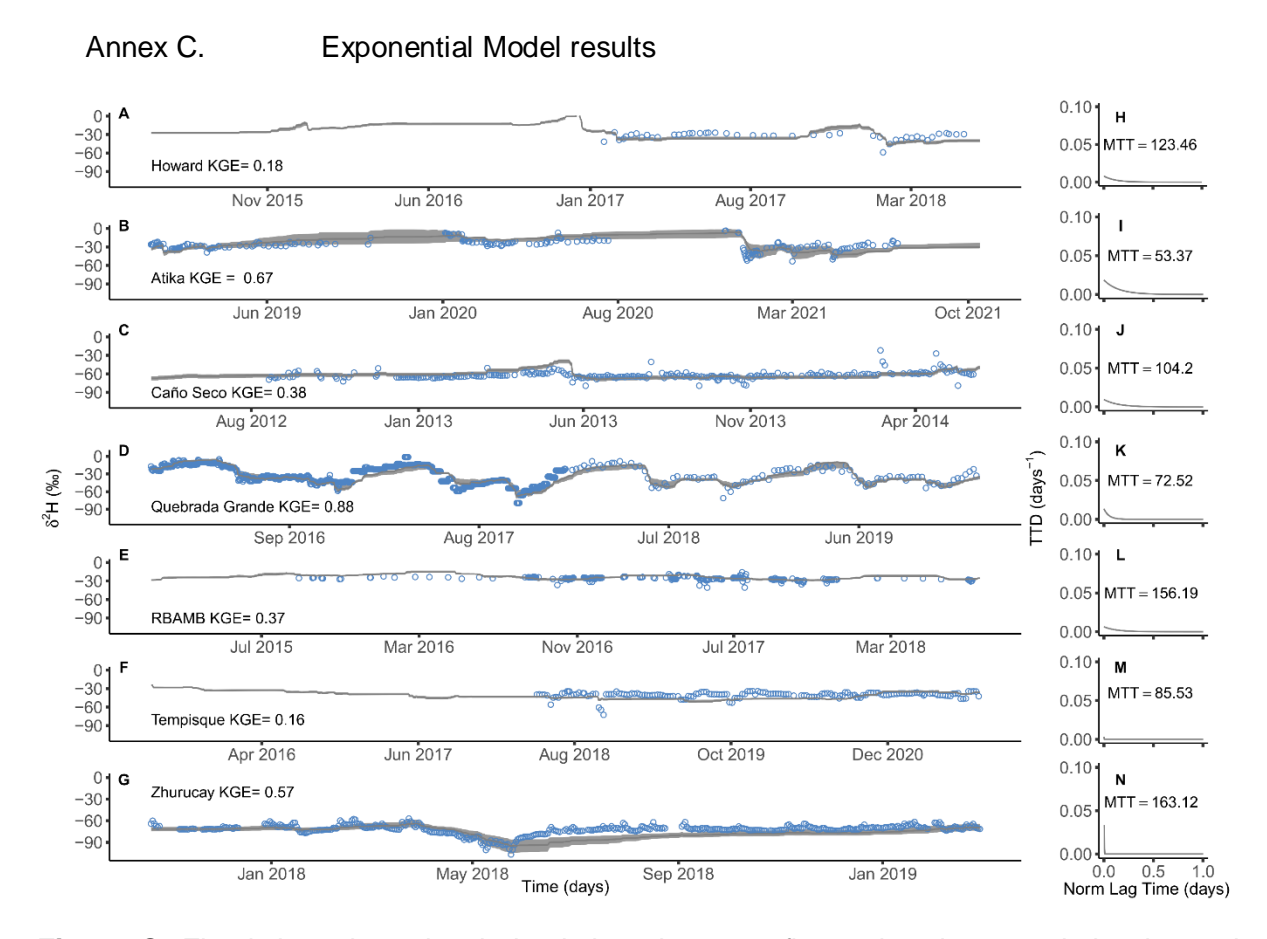


**Figure C.** Fitted deuterium signal simulations in streamflow using the convolution integral approach with exponential model as transference function: A-G: Deuterium signal simulations in streamflow. Isotopic signal of the streamflow in blue points. 90% uncertainty bands obtained from the isotopic signal of the precipitation are in gray color. H-N: Probability Density Functions (PDF plotted with the best MTTs values) in gray line.



Annex D. Correlation assumption

**Table D.** Speaman's correlations assumptions. Linearity with the mean of the residuals equal or around to zero as valid. Normality with p-value > 0.05 with a valid hypothesis Ho: The residuals have a normal distribution. Homoscedasticity with p-value > 0.05 with a valid hypothesis Ho: The variance of the errors is the same for any combination of values of the independent variables. Independency with p-value > 0.05 with a valid hypothesis Ho: The linear regression residuals are uncorrelated.

Correlations	Linearity	Normality	Homoscedasticity	Independency
	Mean residual	p-value > 0.05	p-value > 0.05	p-value > 0.05
MTT-Andosols	-5.07e-15	0.93	0.39	0.10
MTT-Igneous	-2.03e-15	0.48	0.28	0.56
MTT-Sedimentary	-9.53e-16	0.14	0.26	0.81
MTT-Precipitation	-1.42e-14	0.22	0.33	0.79
MTT-Delta Storage	5.08e-16	0.23	0.47	0.74
MTT-Seasonality Index	3.04e-15	0.18	0.21	0.13
MTT-Day0	-6.08e-15	0.61	0.74	0.36
Alpha-Andosols	9.92e-19	0.66	0.23	0.53
Alpha-A(Sa)	9.93e-19	0.48	0.20	0.64
Alpha-Altitude	-5.94e-18	0.001	0.83	0.70
Alpha-AET	-6.93e-18	0.12	0.84	0.61
Alpha-Month0	6.93e-18	0.47	0.33	0.38
Alpha-PMVAR	-9.93e-19	0.99	0.34	0.92